User's Guide to the Grand Canyon Ecosystem Model

Prepared for:

By:

Josh Korman
Ecometric Research Inc.
3320 W 5th Ave.
Vancouver, B.C.
Canada, V6R 1R7

Carl Walters
University of British Columbia
Fisheries Centre, 2204 Main Mall
Vancouver B.C.
Canada, V6T1Z4

September 28, 1998

Acknowledgements

Development of this model relied on the involvement of scientists and managers with experience in the Grand Canyon. Contributors include:

Physcial Sciences

Ted Melis, Tim Randle, Bill Jackson, Stephen Wiele, David Topping, Joe Hazel, Matt Kaplinski, Randy Peterson, Terry Fulp, Mark Anderson, Rod Parnell, Roger Pulwarty, Bill Vernieu, Susan Huefftle, Jeanne Korn, Jim Smith, Eleanor Griffin, Jim Bennett.

Biological Sciences

Barry Gold, Larry Stevens, Barbara Ralston, Mike Yard , Rich Valdez, Bill Persons, Michael Kearsely, Michael Douglas, Joseph Shannon, Owen Gorman, John Spence, Tim Hoffnagle.

Socio-Economics and Cultural Resources

Dave Garrett, David Harpman, Ruth Lambert, Clayton Palmer, Wayne Cook, Andre Potochnik, Kerry Christensen, Mike Yeatts, Richard Hereford, Robert Winfree, Dave Foster, Barbara Foster.

Table of Contents

1.0   Introduction

The primary objective of developing the **G**rand **C**anyon Ecosystem **M**odel (GCM) was not to create a simulation program that permits detailed quantitative predictions about the effects of changes in management of Glen Canyon Dam on downstream resources, but one that helps define and priorize research programs and experimental monitoring design. The main premise of Adaptive Management is that our knowledge of an ecosystem is generally not sufficient to predict how it will respond to various management actions, thus we must manipulate the system and observe its response. However, such management experiments are potentially risky and expensive and responses can be difficult to measure. Thus, we must do as much as possible to develop a sound and simplified experimental design.

The development of a computer model can assist in the design of an experimental management and monitoring plan. First, just trying to build an explicit numerical model exposes broad gaps in data and understanding that are easy to overlook in verbal and qualitative assessments and tells you where you need to focus your research and monitoring. Second, we have found that even quite crude models can help greatly to "screen" policy options so as to eliminate options that are simply too small in scale to be effective, or would be extremely risky given uncertainty about even directions of response in key policy indicators. It can also help eliminate certain hypotheses of system response or behaviour if they can't be reproduced in the model. Lots of ideas you can get away with on paper don't pan out when you try to represent them clearly enough via a computer algorithm. Finally, while predictions may be approximate, they provide indications of resource trade-offs and long term variability in key indictors. Viewing this kind of output is educational for many, and required thinking when designing an experimental management program.

This user's guide is structured into three components. Section 2.0 describes how to download the program from the INTERNET and install it on a personal computer. Section 3.0 describes how to use the program, that is, control the simulations and use the dialogue boxes to modify parameters, adjust graphics, and save results. Section 4.0 describes the model's structure and assumptions.

2.0   Downloading and Installing the Software

GCM can be run on a PC with a 32-bit operating system, such as Windows 95 or Windows NT. The GCM installation program can be downloaded from the GCMRC Web or FTP servers. To download the model from their Web site, go to the GCMRC home page (http://www.usbr.gov/gces/) and move to the Conceptual Modelling link. Download gcmsetup.exe from the Download Model choice. To download the model from their FTP site, logon anonymously to 140.217.15.114 and download gcmsetup.exe from the /pub/model directory.

Gcmsetup.exe is a self-extracting WinZip archive file. Download it to a temporary directory on your hard disk and double-click on it from the Windows Explorer to extract the files. When you have done this, double-click on setup.exe (one of the extracted files) to initiate the installation program. After installation is complete you can delete the contents of the temporary directory.

3.0   Using the Program

The Grand Canyon Ecosystem Model consists of four parts: (1) data management routines for entering historical "driving" information on water flows and sediment, and reference biophysical data for comparison with model predictions (Microsoft EXCEL files); (2) graphics display routines for storing and displaying simulation results in various formats (time plots, spatial maps, and downstream and cross-section profiles); (3) a simulation control system (several menus and display windows) for defining scenarios (policy variable choices, biophysical parameter choices) and controlling simulation runs; and (4) a set of submodels for dynamic changes in key parts of the ecosystem. This section of the user's guide describes items 2) and 3) above. Section 4.0 provides descriptions of submodel structure and assumptions.

To start GCM, double click on the file gcm.exe from the Windows Explorer. After some initial files are loaded, a graphical user interface will appear with a menu on top of the main window or form, a series of graphs showing simulation results for selected model indicators, and a series of model controls in the lower portion of the main window.

3.1   Controlling the Simulation – The "Controls and Model Progress" Frame

The main controls for the model are located in the "Controls and Model Progress" frame at the bottom main window. Results for only one selected reach are displayed in the time series graphs. To change this reach, select the new reach from the dropdown list box on the right side of the frame. Set the length of the simulation period from the "Number of years to simulate" text box. The default simulation period is 50 years (1948-1997). Change the value in the text box entitled "Start Yr." if you want to begin a simulation at a later date.

Click on the "Start" button to begin a simulation. To temporarily suspend model execution click on the "Pause" button. While the model is paused you can change parameter values or management actions or graphics. To resume execution, click on the "Continue" button. To stop a simulation completely in order to restart from the start year, click on the "Stop" button. The "Pause at end of year" option automatically pauses the model after each simulation year is complete. The "Overlay results" option allows you to compare the previous simulation's results with values from a new run. To use this option, complete the first simulation then click on the "Overlay results" check box, modify any parameters or management actions, and click on the "Start" button to begin the second simulation. The original simulation results will be displayed by lines, while the more recent simulation results will be displayed by filled circle symbols.

3.2 Controlling Graphical Output – The "Set Graphics" and "Legend Editor" Dialogue Boxes

The "Set Graphics" dialogue box, accessed under the "View" main menu item, controls the type and format of graphics which display model results. Four types of graphics are available:

1) time series graphs showing results over time for a single reach (that the user specifies in the "Controls and Model Progress" frame) – **"Graphs"** Tab;
2) Maps, where results from all reaches for a single timestep can be viewed at once in map format by using colors to denote the indicator values in each reach – **"Maps"** Tab;
3) Downstream concentration profiles, where results from all reaches for a single timestep can be viewed at once in bar chart format – **"DS Profiles"** Tab; and
4) Cross-Section Profiles, where detailed results for a few indicators (sand storage, algae, riparian vegetation) are displayed for all reaches in a single timestep. These profiles show the value within each 2 ft depth slice (see Section 4.1) and colors are used to denote the indicator values **– "Cross Section Profiles"** Tab.

To view each type of output, you must check the appropriate check box on the "Visible Forms" frame on the "Graphs" tab. You can view up to six panes for the first three types of graphical outputs and up to 3 cross-section profiles. To determine how many panes to view for each graph type, check or uncheck the "visible" text box beside the dropdown combo box for each pane. The indicator to be displayed in each pane is set by selecting from a set of all possible indicators (40 in the current version of GCM) in the dropdown combo boxes. For times series graphs and downstream profiles, the Y axis minimum and maximum values can vary dynamically over the coarse of the simulation or can be fixed if you specify values in the Y axis min. and max. text boxes on the "Graphs" and "DS Profiles" tabs.

Parameters under the "Settings" frame on the "Graph" tab allow you to further adjust the graphical output. For time series graphs, you can adjust the number of years shown in each graph so you can see seasonal patterns (set the value low) or long-term patterns (set the value to the number of years you are simulating). Observed data can be displayed as long-term averages or as individual monthly (or annual for some indicators) values. For maps and downstream profiles, you can update the output each month of the simulation or only once per year for a specific calender month. If you specify a set of graphs and Y-axis conditions in the "Graphs" tab, you can replicate this configuration for the downstream profiles by clicking on the "Sync Graphs and DS Profiles" button on the "Graphs" tab.

When viewing model output some indicators will contain multiple lines. For example, the discharge indicator shows the minimum and maximum discharge in each reach for each month of the simulation. In the main window, double click on a graph to view its line legend. For plots comparing predictions with observed data, predictions are denoted by red lines while observed data are shown as blue dots (time series graphs) or lines (downstream concentration profiles).

The "Legend Editor" dialogue box, accessed under the "View" main menu item, allows you to control the color legends used on the maps and cross-section profile graphics. For each model indicator, you can specify whether you want a continuous or categorical

color range. With a continuous range, 50 colors will be used to represent the range of values between a minimum and maximum that you specify. For a categorical display, you specify the number of categories to use, and set the upper and lower limits for the range. When you press on the return key after clicking on the "Number of Categories" text box, the break points for each range and color selection will be automatically populated. If you wish to change the colors for a particular range, click on the new color in the color pallete and then click on the color box beside the category in the "Categorical Map Scale" frame. You can manually edit the breakpoints as well. When you exit the dialogue box via the "OK" or "Apply/Save" buttons, any changes you make to the map legend are automatically saved to the file which stores this information (model.mde) and will be available for subsequent modelling sessions.

3.3   *Saving Model Parameters, Management Scenarios, and Model Results*

There are a large number of parameters controlling model performance and output that can be adjusted by the user. To save any modifications you make in one session to reuse in a subsequent session, you must save the parameters to the appropriate file and load this file in the subsequent session. The file loading and saving routines are accessed from the "File" main menu item:

Load/Save Graphics Setup File
Saves or restores all parameters controlling simulation output (what type of output, how many panes, what indicators,…)

Load/Save Physical Submodel Parameters
Saves or restores all parameters controlling the sediment budget (set from the "Sediment Budget" dialogue box).

Load/Save Chemistry/Production Submodel Parameters
Saves or restores all parameters controlling oxygen concentrations, benthic algae, and aquatic-based detritus and insect production (set from the "Aquatic Production" dialogue box).

Load/Save Population Submodel Parameters
Saves or restores all parameters controlling the fish and bird population models. This includes population dynamics, and habitat and trophic linkages.

Load/Save Tributary Habitat Data
Saves and restores relationships between ponded tributary rearing area and backwater areas and discharge for each reach specified by the user in the Animal Populations – "Tributary/Backwater Habitat" dialogue box.

Load/Save Recreation Submodel Parameters
Saves and restores parameters controlling white water rafting use and angling.

Load/Save GCD Experimental Release Sequence
Saves and restores variables determining: a) which years are experimental temperature years (subject to temperature modification); b) the extent of temperature modification in each month (specified from the "Set GCD Outflow Temperature" dialogue box); and c) the type of diurnal flow regime (e.g. No Action, Steady,…) for each year of the simulation

(specified from the "Set Annual Sequence of Diurnal Patterns" tab in the "Set GCD Release Hydrograph (Diurnal/Spike)" dialogue box).

Dump Results
Following a simulation, results can be exported to a comma-delimited ASCII file. Selecting the "Dump Results" submenu item will bring up a dialogue box prompting you to specify which model indicators you wish to save. You must also specify which reaches you wish to save results for.

3.4 "Set GCD Release Hydrograph (Diurnal/Spike)" Dialogue Box

The "Set GCD Release Hydrograph" dialogue box, accessed via the "Policies" main menu item, allows the user to adjust diurnal discharge regimes and spike flows (AKA beach habitat building flows). The dialogue box consists of three tabs.

"Diurnal Pattern" Tab

Diurnal discharge regimes which can be currently simulated in GCM include the Modified Low Fluctuating Flow (MLFFA), No Action, Interim, and Steady flow alternatives. Reach-specific hydrographs for each of these regimes are pre-computed via the Peakshave and USGS unsteady flow models for a range of monthly release volumes from GCD for each calender month. These results are saved to files (with *.sts extensions) which are read-in by GCM each time the diurnal flow regime is changed during a simulation.

The diurnal flow regimes are specified by a series of flow constraint parameters shown in the dialogue box (minimum and maximum daily flow, maximum daily flow change, upramp and downramp rates). To view these parameters and the resulting typical diurnal patterns (during on- and off-peak demand periods), click on any of the filenames in the "Release Scenarios" list box in the upper left corner of the tab. The 24-hour hydrograph will vary with the calender month, release volume, and reach and user's can select alternate combinations of these factors to view how they effect typical discharge regimes. In the upper right corner of the tab, the "power value" shows the value of electrical power generated from GCD in 1996 dollars based on the currently selected month and release volume. The "monthly loss" value represents the difference in the electrical power generation value between the currently selected release scenario (e.g. MLFFA) and the No Action scenario for the specified month and release volume. The "annual loss" value represents the power generation value difference between the currently selected release scenario and the No Action alternative for a typical year (in terms of release volumes by calender month).

To create a new diurnal discharge regime scenario, modify any of the flow constraint parameters (you can use the copy, paste, delete buttons on the right side of the tab to make this task easier), specify a filename to save results to in the lower right corner of the dialogue box, and click on the **"process"** button. This will cause GCM to run the PEAKSHAVE and USGS unsteady flow models (see Section 4.2) for each calender and release volume combination (typical processing time 1 hr). When the processing is complete you can view the results by clicking on the new file name in the "Release Scenarios" file list box. To use this new scenario in future simulations, you must exit GCM, manually edit the file diurnal_scenarios.txt file to include the name of the new scenario that you just created, and restart the program. Then go to the "Set Annual

Sequence of Diurnal Patterns" tab of the "Set GCD Release Hydrograph" Dialogue box and include this scenario for some/all years of the simulation as described below.

"Set Annual Sequence of Diurnal Patterns" Tab

Each simulation year must have a diurnal flow regime associated with it. By default, GCM uses the historical pattern: 48-63=steady flow (no diurnal variation), 63-90=No Action, 91-96=Interim, 97+=MLFFA. To change this sequence, simply click on the regime in the upper left corner of the tab, and then click on the cell(s) for the specific year(s) to be associated with this regime in the adjacent table. When you click on cells in the table, you will see that the numeric code for the regime you selected will replace the current code for the selected cell(s).

"Spike Flows" Tab

The duration and magnitude of spike flows are set by adjusting the parameters in the upper left corner of this tab. The required volume (in acre-feet) is displayed each time these values are adjusted. The frequency of spike flows can be set manually or automatically. The manual or "User-defined Implementation" option allows you to search through the release volumes for each month of the simulation period (by typing a new year and month in the appropriate text boxes or cycling through them via the spin buttons) to find values that exceed the volume required for the spike you specified. Click on the "Add to List of Spikes" button to add a particular year-month combination to the spike list at the bottom of the tab. Any year-months in this list will cause the model to implement a spike flow during the simulation. The alternate method of spike flow implementation is to only allow spikes in months where Riverware simulations have specified they can occur based on the beach habitat building flow triggering criteria. To use this option, you must first load a Riverware run with a spike flow of fixed magnitude (200, 238, 297, 357 KAF) from the "Set Monthly GCD Hydrograph/Tributary Flow" dialogue box via the "Monthly Release Sequence from GCD" dropdown combo box. When you click on the "Riweare spike flow implementation…" option from the "Spike Flows" tab, the magnitude of the spike flow will change to reflect the value used in the Riverware simulations, and the years where the triggering criteria allowed a spike flow will be shown in the list box. You can add or delete any year-month combinations from this list.

3.5 *"Set GCD Monthly Hydrograph/Tributary Flow" Dialogue Box*

The "Set GCD Monthly Hydrograph/Tributary Flow" dialogue box, accessed via the "Policies" main menu item, allows you to control monthly release hydrographs from GCD and modify hydrographs from major tributaries below GCD (Paria and Little Colorado Rivers). By default, the model uses the historical GCD release sequence for the post-impoundment period, historic monthly volumes past Lees Ferry for the pre-impoundment period, and historic monthly average discharges for the Paria and LCR hydrographs. To view the current hydrograph select GCD, Paria, or LCR from the dropdown combo box in the upper left corner of the dialogue box. The hydrograph will be displayed in the adjacent graphic as monthly release volumes (GCD) or average monthly discharge (Paria and LCR). You can change the Y axis maximum of the graphic via the text box at the top of the Y axis (you must press the return key for the change to take effect).

There are three basic monthly release options that can be defined for GCD and are set by the radio buttons below the hydrograph graphic:

Historic/Riverware Option
When this option is selected, you can use the historic release volume or 5 different Riverware scenarios selected from the "Monthly release sequence from GCD" dropdown combo box. The Riverware scenarios include the base case and 4 different spike flows implemented via the BHBF triggering criteria (200, 238, 297, 357 KAF). For each Riverware scenario, you can select one of 10 hydrologic traces.

User Defined Monthly Sequence One Year
When this option is selected, you must set the monthly release sequence for one year by drawing on the graphic at the top of the dialogue box. First set the Y axis maximum, and then draw the hydrograph by holding the left mouse button down while dragging the mouse over the graphic. This pattern will be repeated each year of the simulation, thereby eliminating any interannual variability in GCD releases. This option is useful for exploring model behaviour.

Simulation of flow regimes like the Seasonally Adjusted Steady Flow (SASF) alternative involves changes to monthly water scheduling at GCD but such changes must consider upper and lower basin water demands and other factors effecting operations of the Colorado River Storage Project. In theory, any change to current operations to be simulated in GCM should be implemented by specifying the flow regime to BOR who will then run the scenario through their Riveware model to produce a monthly release sequence which can be read-in by GCM. In consultation with BOR, we have provided a "quick-and-dirty" option for examining alternatives like SASF without having to go through all these steps, thereby facilitating interactive gaming with the model. The idea is that user's specify a relative pattern of monthly releases (by drawing on the graphic at the top of the dialogue box). As the simulation proceeds, the annual release volume (historic or Riverware defined) is conserved, but the monthly releases are determined from relative pattern defined by the user (the sum of monthly releases over the year will equal the annual volume). However, such changes can only occur in relative low water years when flood control issues do not dominate reservoir operations. To implement this option, click on the "relative pattern in monthly release volumes" check box in the "GCD Seasonal Monthly Release" frame (which is only active when the "user defined monthly sequence for one year" option is selected). Specify the maximum annual release volume when the relative pattern will be applied and then draw the relative monthly release pattern. As the simulation proceeds, historical or Riverware defined release volumes will be used when the total annual volume exceeds the maximum you specified. In years when the annual volume is less than this value, the user-defined monthly release sequence pattern will be implemented.

Repeat Monthly Sequence for One Year
When this option is selected, a monthly release sequence from one of 50 years (1948-1997), set by the text box adjacent to this radio button option, is repeated for each year of the simulation.

Tributary Hydrographs
By default, the model uses the historic 50 year sequence of average monthly discharges. However, you can repeat a user-defined monthly sequence for one year for all years of the simulation or repeat one of the historic years. When these options are

selected, sediment inputs will be computed from rating curves and the discharge hydrograph you specified.

3.6   "Set GCD Outflow Temperature" Dialogue Box

This dialogue box allows you to adjust outflow temperatures from GCD to simulate the effects of a selective withdrawal structure. The temperature model uses the outflow temperatures from GCD and other parameters specified in this dialogue box to predict mean monthly water temperature in each reach (See Section 4.2.5 and 4.2.6). By default, the historic average monthly release temperatures from GCD are used in the simulation (shown in the "normal" column in he table on the left side of the dialogue box). If you wish to modify the temperature in some months, change the values in the "experimental" column to reflect temperatures that are realistic give typical thermal profiles in the GCD forebay and the depth of selective withdrawal inlets (BOR should be able to provide some advice on feasible temperature ranges by month). The "equilibrium" column represents the theoretical water temperature that water flowing through Grand Canyon could achieve given an infinite amount of time to equlibrate with air temperatures. These are parameters that, in conjunction with the heat exchange rate, have been tuned to fit historic and downstream patterns of temperature change. An examination of predicted and observed mean monthly temperatures in GCM shows that the current parameterization fits the data quite well.

If you have adjusted the mean monthly GCD release temperatures in the "experimental" column, you then need to specify which years of the simulation the experimental temperatures will be implemented in. To do this, click on the desired years in the table on the right side of the dialogue box. You can select multiple cells by clicking on the first cell and then dragging the mouse down the table (across years) while holding the left mouse button down.

3.7   "Sediment Budget and Camping Beach" Dialogue Box

The "Sediment Budget and Camping beach" dialogue box, accessed from the "Parameters" main menu item, contains parameters that effect sediment budget and camping beach availability calculations within GCM. These components of the model are described in Sections 4.2.2 and 4.2.3, respectively.

Sediment Budget Parameters Tab

This tab contains parameters controlling the sediment budget of GCM.

Subsurface Erosion Rate: The proportion of sand mass lost from morphology environments below the water surface.

Eolian/Surface Erosion Rate: The proportion of sand mass lost from morphology environments above the water surface.

Angle of Repose…: Stable slope angle on channel margin deposits (in degrees). Note that the angle of repose and average length of channel margin deposits are used in conjunction with the reach averaged cross-sections and number of channel margin deposits per reach (from air photographs) to compute channel margin storage. If you

change these parameters you must recompute channel margin storage by clicking on the "Recompute Storage" button on the "Storage Potential" Tab.

Average Length of Channel Margin Deposit: Average length of a channel margin deposit (in miles).

Initial Sand Storage: Initial storage for each environment at the start of the simulation can be set to full (=1) or empty (=0) to reflect conditions in the starting year.

Proportion of Sand Inflow…: The proportion of sand entering a reach (from the upstream reach and tributaries) destined to each environment (must sum to one across 3 environments).

Eddy/Channel Margin Storage Potential Change..: The bottom frame of the "Parameters" tab contains parameters and the resulting functional relationship which reduces storage potential in eddy and channel margin 'slices' (Fig. 3) as a function of the of discharge difference (current discharge – discharge that would just inundate the slice). Modification of these parameters updates the curve shown in the graphic. Note that this relationship can be effectively turned off in the model by setting the "KCFS difference when storage potential is reduced by 50%" parameter to a large value (e.g. 300).

Storage Potential Tab

This tab shows reach-specific potential storage-discharge relationships. The table below the storage-discharge curves can either display morphology statistics for each reach (number of eddies and channel margin deposits) estimated by air photographs and used to compute the storage-discharge curves, or the storage potential at a user-defined discharge level. Morphology statistics or storage can be standardized by the length of each reach to facilitate comparison among reaches. Note that this table is for summary purposes only and you cannot modify any its values.

Camping Beaches Tab

This tab contains parameters controlling predictions of beach numbers in each reach by size class as a function of sand storage and eddies.

Stage Range for Beaches: The minimum and maximum stage (in cfs) of camping beaches. The index of sand storage in eddies (relative eddy fullness, see next parameter) used to predict the number of beaches is computed within this stage range only.

Base Relative Eddy Fullness within…: A relative value ranging from 0 to 1 which represents the extent of sand storage in eddies within the camping beach stage range only (0=completely empty, 1=completely full). This value should reflect the extent of sand storage during the period when the camping beach inventory (shown in table) was taken (1991 in the current version of GCM).

Campsite Inventory Table: The number of large, medium, and small beaches in each reach. These data in the current version of GCM are from the 1991 camping beach inventory (Kearsely and Warren, 1992). Click on a particular reach-beach size class cell

in the table to examine the corresponding beach-eddy fullness relation in the adjacent graphic.

Beach-Eddy Fullness Graphic: The relationship between the number of beaches in a reach-beach size class combination and the ratio of eddy fullness (0-1, in beach stage range only), to the base level of fullness (Base Relative Eddy Fullness within… parameter defined above). The number of beaches at a ratio (x-value) of one should equal the number shown in the camping beach inventory (table). To adjust these relations, pick the appropriate reach-beach size class combination by clicking on the corresponding cell in the inventory table. Adjust the y-axis maximum in the graphic (the maximum number of beaches for this reach-size class combination). Then click on the graphic and hold the left mouse button down while dragging the pointer across the graphic.

3.8 "Aquatic Production" Dialogue Box

The "Aquatic Production" dialogue box, accessed from the "Parameters" main menu item, allows users to view and adjust parameters controlling oxygen (Section 4.2.6) and detritus concentrations (Section 4.3.1), primary production (Section 4.3.1), and benthic insect dynamics (Section 4.3.3).

<u>Oxygen</u>

Gameson-Robertson Oxygen Parameters: Parameters from the Gameson-Robertson Oxygen saturation model, assuming salinity=1:

$$Oxygen\ Saturation = (OxPar1 - OxPar2 * 1) / (OxPar3 + Temperature)$$

Lake Powell Outflow O$_2$: Concentration of oxygen in water released from GCD in mg/L.

Oxygen Exchange Coeff: Parameter used to predict the downstream of change in oxygen concentrations (v in Eqn. 4.2.1).

<u>Primary Production</u>

Base Light Extinct. Constant of the relationship predicting light extinction as a function of suspended sediment concentration (in mg/L). Equivalent to the light extinction when suspended sediment concentration = 0 mg/L.

Light Extinc/turbidity: Slope of the relationship predicting light extinction as a function of suspended sediment concentration (in mg/L).

Fine Weighting: Constant used to determine how fine (< 0.0625 mm) and sand material is used in the light extinction equation. When the value is less than zero, fine and sand concentrations are simply summed. If the value is one, the suspended sediment concentration used in the relation is the average concentration of fine and sand material. Increase the value to >1 to have light exctinction change more with variation in fines than sand (fine material has a greater surface area/wgt than sand and therefore is more effective at attenuating light).

Maximum algae biomass: The maximum possible equilibrium biomass for benthic algae (Cladophera) in grams AFDM/ft^2.

Photosynth. Effic.: Photosynthetic efficiency, the ratio of mortality to the maximum photosynthetic rate. The larger this value, the smaller the resulting algal biomass for a given light intensity.

Detritus

Tributary Detritus: Average detritus concentration from tributaries in grams carbon (AFDM) per m^3.

Lake Powell Detritus: Average detritus concentration in GCD outflow in grams carbon (AFDM) per m^3.

Nat. System Detritus: Average detritus concentration in Glen Canyon prior to impoundment in grams carbon (AFDM) per m^3.

Terrestrial Detritus…: Detritus (grams carbon AFDM) produced per unit of basin area (m2) during a spate (defined as a storm with >1 in. rainfall).

Detritus produced from Algae: Total amount of detritus produced (grams carbon AFDM) per unit of bottom substrate (m2) per unit of benthic algae (grams carbon AFDM per ft^2 of bottom).

Detritus Sinking Rate: Loss rate of labile detritus due to bacterial decomposition, expressed in ft/day (v in Eqn. 4.2.1). To convert this loss rate to a turnover rate:

Turnover rate (proportion consumed/day)= sinking rate (ft/day)/water depth (ft)

For example, a sinking rate of 0.5 ft/day is equivalent to a daily turnover rate (proportion consumed per day) of 2.5% (0.025) assuming an average depth of 20 ft.

Labile Prop. Algae Detritus: Proportion of detritus from algae that is labile.

Labile Prop. Terrest. Detritus: Proportion of detritus from terrestrial sources (riparian vegetation and basin-spate inputs) that is labile.

Detritus Consumed by Benthos: Loss rate of detritus (expressed in ft/day) per unit of benthos (expressed as grams carbon AFDM per m^2 of bottom). See detritus sinking rate description for details of converting ft/day loss rate to a turnover rate.

Decomp./sink Rate, Refract. Detritus: Total loss rate of refractory detritus due to decomposition and sinking (ft/day). See detritus sinking rate description for details of converting ft/day loss rate to a turnover rate (v in Eqn. 4.2.1).

Benthic Insect Dynamics

Avg. Glen Canyon Detritus for Initialization of Benthos: Detritus concentration (labile and non-labile) in Lees Ferry Reach used to initialize benthos model (grams carbon AFDM per m^2).

Base Biomass/area below Powell: Typical benthos biomass (grams AFDM/m^2) in Lees Ferry Reach used to initialize the model.

Growth Efficiency: Proportion of labile carbon ingested by benthos that is converted into benthos tissue (e in Eqn. 4.3.10).

Base Biomass Loss/Month: Base mortality rate of benthos (proportion lost/month) due to natural factors (physiology/emergence) and predation on invertebrates not modelled in GCM (see "Trophic Linkages" dialogue box).

Q10 for Temperature Mort Effect: Power term used to increase base mortality rate as temperature increases ($Mort_{total} = Mort_{base} * (Temperature/10)^{Q10}$). A value of 0 implies that mortality will not increase with temperature.

Ratio of Max. Pop. Growth…: The ratio of the maximum population growth rate to base mortality. This parameter is used in GCM to limit the maximum rate of biomass gain over a timestep (month) which is a function of colonization, natural mortality, growth effeciency, and food supply.

Colonization Rate…: Rate of new benthic invertebrate recruitment (grams AFDM/m^2) to each reach from sources outside of the reach.

Relative Availability of Algae/Diatoms: The proportion of total algae biomass available for consumption by grazers.

Diurnal Drying Loss Rate: Power term used to predict the benthic biomass loss rate due to diurnal variation in flow. The ratio of minimum width/maximum width, raised to the power of this parameter (par) determines the relative reduction in biomass:

$$Biomass_{t+1} = Biomass_t * (Width_{min}/Width_{max})^{par}$$

Drift

Powell Drift Concentration: Concentration of drift (grams AFDM/m^3) in outflow from GCD.

Nat. System Drift, Powell: Concentration of drift (grams AFDM/m^3) in Glen Canyon prior to construction of GCD.

Drift Rate: Grams of drift produced (AFDM) per gram of benthos (AFDM) per m^2 of substrate per day.

Drift Sinking Rate: Loss rate of drift expressed as ft/day. See detritus sinking rate description for details of converting ft/day loss rate to a turnover rate (*v* in Eqn. 4.2.1).

3.9 "Riparian Vegetation" Dialogue Box

The "Riparian Vegetation" dialogue box, accessed from the "Parameters" main menu item, allows user's to control biomass dynamics of riparian vegetation See Section 4.3.2 for details of this submodel.

Growth: Intrinsic rate of biomass increase (0=no growth, 1 = doubling of biomass per month assuming no competition). "r_p" in eqn. 4.3.7.

Bug Prd: Biomass of terrestrial insects (grams carbon AFDM) produced per gram of plant per ft^2 of substrate.

Detr. Prd: Biomass of detritus produced from plants (grams carbon AFDM) per gram of plant per ft^2 of substrate.

Min, Max: Minimum and maximum elevation (ft) that the plant community can survive relative to the water table elevation. During a model timestep, if the water table elevation is outside the specified range, biomass will be reduced by 5%.

Dkill: Sensitivity of the plant community to flooding (0=can withstand constant inundation). During each model timestep, the product of **Dkill** and water depth over a slice determines the x-axis value in the Flooding-Mortality matrix (see parameter description below).

Mort vs. cum dkill*depth (Flooding-Mortality Matrix): Proportion mortality (0-1 on y-axis) as a function of the product of sensitivity to flooding (**Dkill**) and depth of flooding (x-axis). Note that this product is summed across all timesteps while the slice is inundated (see **Dkill** description).

Competition Matrix: Competition coefficients of one plant community on another. Explicitly, it is the effect of a unit of biomass of plant type k on the growth rate and carrying capacity for plant type p (see Eqn. 4.3.7).

Substrate Matrix: Substrate size classes that support different community types. To change the matrix, click on the present or absent green and red boxes and then click on the appropriate cell in the matrix.

3.10 "Population Dynamics Parameters" Dialogue Box

The "Population Dynamic Parameters" dialogue box is accessed via the "Animal Populations" sub-menu below the "Parameter" main menu item. User's are instructed to review Section 4.4 of this report to understand how the following parameters are used.

Dispersal: Proportion of animals remaining in their natal reach each year. This value controls the extent of redistribution of animals between reaches based on the ratio of predation to food availability (P/F) in each reach. If the dispersal value is high there is little redistribution, implying that spatial patterns of abundance are largely controlled by reach-specific physical features (e.g. LCR for Humpback chub).

Wt mat: Body weight at maturity in kilograms.

Max wt mat: Maximum body weight at maturity (in kilograms) which occurs when population densities are low (when competition is reduced).

Rho: Growth parameter defining the slope of a Ford-Walford plot (weight of age + 1 vs. age).

Survival (age 1+): Adult (mature animals only) annual survival rate, expressed as the proportion surviving.

Juv. Surv (age 1+): Annual survival rate for animals age 1 – age at maturity, expressed as the proportion surviving.

Age mat: Age of maturity in years.

Eggs/k: Fecundity, expressed at the number of eggs per kilogram of mature animal.

Sfry: Egg-to-fry survival rate, expressed as the proportion surviving

Sjuv: Fry-to-age 1 survival rate, expressed as the proportion surviving.

Comp K: The ratio of maximum survival rate at very low population density to the survival rate for a balanced population. There are no empirical data on K* for Grand Canyon vertebrates (no stock-recruitment data); but based on comparative studies of fish recruitment relationships (Myers and Barrowman 1996) we advise users to assume values on order 3-10. This ratio replaces the need to specify values of **Sfry** and **Sjuv**.

Ppred: Proportion of egg-to-fry mortality due to incidental predation.

Reach: Reach number where majority of incidental predation mortality occurs (2=GCD-Lees Ferry).

Wk1 and Wk2: Calender month window when majority of incidental predation occurs.

Vol Power: Predation dilution parameter that simulates the effect of prey concentration during low flow periods. If value=0, predation will not scale with flow. If value=0.5, predation mortality will scale with wetted area. If value=1, predation will scale with discharge volume.

3.11 "Habitat Linkage Relationships" Dialogue Box

The "Habitat Linkage Relationships" dialogue box is accessed via the "Animal Populations" sub-menu below the "Parameter" main menu item. This dialogue box allows users to specify linkages between various habitat conditions and food availability, habitat area, predation, and growth. User's are instructed to review Section 4.4 of this report to understand how the following parameters are used.

Select the animal to define habitat linkages for from the dropdown combo box at the top of the dialogue box. For the appropriate habitat variable and effect combination (e.g. the effect of temperature on predation), sketch in the relationship between the magnitude of the effect (y-axis) and the value of the habitat variable (x-axis). To sketch the relationship, hold the left mouse button down and drag the mouse across the graphic. The x-axis is dimensionless and represents the relative range of a particular habitat value. The vertical arrow below the x-axis represents the habitat value at the 1993 baseline condition (when the population is assumed to be stable). The arrow can be dragged to the appropriate position on the x-axis and is used to scale this axis. If habitat conditions remained at 1993 levels, the population would remain stable, but if they change, food availability, habitat area (column 1), predation (column 2), and growth (column 3) will change according to the function(s) you specify. For example, you might specify a temperature-predation relationship for Humpback chub (increasing temperature decreases predation), where a 10% increase in temperature relative to 1993 values reduces predation by 20%, while a 50% temperature increase reduces predation by 75%.

The bottom sketch graphic describes how sensitivity to predation and food availability varies with juvenile age. Presumably vulnerability to these effects is maximum when the animals are young and unable to withstand long periods without food or move to areas with higher food availability or less predators.

The "Set reach capacities using habitat relationships only" check box allows you to see if the explicitly recognized habitat relationships you defined can explain observed spatial distribution patterns (see Section 4.4.1) by comparing predicted and observed abundances over time using the downstream profile graphics.

3.12 "Tributary/Backwater Habitat" Dialogue Box

The "Tributary/Backwater Habitat" dialogue box is accessed via the "Animal Populations" sub-menu below the "Parameter" main menu item. This dialogue box allows you to sketch in hypsometric relations between tributary and backwater rearing area and discharge for each reach. In the absence of map-derived values, these relations are currently sketched in by the user but can be replaced by more accurate relationships when they become available.

Total tributary rearing area is defined by setting the total length of accessible tributaries for each reach and how the useable width varies as a function tributary discharge. The total area of ponded tributary rearing area is sketched in as a function of mainstem discharge, as is the average size of backwater rearing areas. Total backwater rearing area for a reach is computed by multiplying the average area for a given discharge by the number of backwaters in the reach.

3.13 "Trophic Linkages" Dialogue Box

The "Trophic Linkages"' dialogue box, accessed via the "Animal Populations" sub-menu below the "Parameter" main menu item, allows the user to modify predator prey relationships used in GCM. The dialogue box contains two frames with a list of all animal populations simulated in the model. One frame represents the animals as prey and the other represents them as predators. Lines between any two animals (e.g. Humpback chub as prey and channel catfish as predators) indicates a preday-prey relationship. If you select a particular combination by clicking on radio buttons in the prey and predator frames, the proportion of prey mortality associated with the predator is displayed, as is the proportion of the predator's diet contributed by this predator type. Note this dialogue box also shows relationships between animal populations and the food base (terrestrial insects, Cladophera, aquatic insects).

3.14 "Trout Angling" Dialogue Box

The "Trout Angling" dialogue box, accessed from the "Recreation" sub-menu below the Parameters" main menu item, allows users to adjust parameters controlling fishing effort and catchability effecting the trout angling submodel of GCM. See Section 4.5.3 for a description of this submodel.

Catchability: The maximum proportion of the total biomass of vulnerable fish caught for a single unit of effort (i.e. one angling day). For example, if the Lees Ferry Reach vulnerable trout population is 100,000 fish or approximately 100,000 kg, and a maximum of 20 fish (or kg) are caught in one angler day, maximum catchabitlity = 20/100,000 = 0.0002.

Vulnerability-Age Table: For each age, these parameters are multiplied by the maximum catchability value to estimate the age-specific vulnerability (i.e. a value of 0.1 represents a catchability that is 10% of the maximum value).

Total Angling Days in Year: The maximum number of angling days over the year from GCD to the bottom of the last simulated reach (downstream of Diamond Creek).

$ Spent Locally Per Angler Day: Monthly estimates of the dollars spent in Lees Ferry per angler day (gas, food, hotel). The product of these values and the predicted (or user-defined) angling days per month in the Lees Ferry reach is the direct economic benefit of angling predicted within GCM.

Distribution of Effort Table: A monthly table of multipliers used to distribute the total number of angler days per year among reaches. All values in this table must sum to one.

Relative Catchability and Effort Table: The first column represents a multiplier describing how catchability changes across seasons (a value of 0.5 for one month suggests that catchability is 50% of the maximum **Catchability** value). The second column represents the relative distribution of effort among months (these values must sum to one).

Annual Effort Responds to Vulnerable Biomass: Flag which allows effort to vary dynamically as a function of the current biomass of fish that are vulnerable (relative to

the 1993 vulnerable biomass)rather than remaining fixed at the **"Total Angling Days in Year" (see eqn. 4.5.2)**.

Relative Vulnerable Biomass…: Ratio of biomass of vulnerable fish during current timestep to the biomass of vulnerable fish in 1993 required to produce 50% of the maximum annual fishing effort (total angling days * maximum value of y-axis of graphic). *RelBio* in eqn. 4.5.2.

Slope: Steepness of effort-vulnerable biomass relationship. *Slope* in eqn. 4.5.2.

Maximum: Y-axis maximum of effort-vulnerable biomass relationship. The absolute maximum is the product of the relative maximum value (e.g. 3) times the **Total Angling Days in Year**. *EffortMax* in eqn. 4.5.2.

3.15 "Rafting Use" Dialogue Box

The "Rafting Use" dialogue box is accessed from the "Recreation-Rafting" sub-menu item below the "Parameters" main menu choice. This dialogue box allows users to view and adjust parameters controlling camping beach use by white water rafters. See Section 4.5.2 for details of this submodel.

When the dialogue box first appears, all the parameters are hidden but two graphs are visible. The left graph shows the demand and availability of campsites by size class and reach for the last complete model month (expressed as the number of campsite days per month = number of campsites available or required * number of days in month). The "campsite use" graph shows the number of nights each campsite in the 1991 campsite inventory was occupied for the last simulated month (the x-axis is the campsite number (1-129 in current database, see "Campsite" sheet in physical.xls to relate campsite number to campsite name/location). Values will range from 0-30 or 31, except in situations where the sites are 'double-booked' (two parties occupying the same beach) when values will exceed the total number of days in the month. Note you can view these graphs as the simulation proceeds. There are two ways to do this. The simplest is to start the simulation and then open the "Rafting Use" dialogue box. Alternatively, open the dialogue box first, click on the "Start" or "Continue" buttons in the "Controls and Model Progress" frame on the main window, and then click on the "Rafting Use Parameters" icon on the Windows taskbar to move the dialogue box on top of the main window.

To view rafting use parameters, click on the "Set Parameters" check box below the graphs. There are four sets of parameters and one output graphic.

Trip Statistic Table: The table showing the number of trips per year, trip duration (nights on river camping), and number of persons on trip for each group type.

Camp Size Class – Group Size Table: The table showing the campsite size class (small, medium, large) required for different group sizes.

Economic Value table: The economic value per individual for commercial (motor and oar) and private rafting trips for each month of the year in 1997 dollars. The total annual value of rafting (excluding day use) is based on the computed number of trips per month, the average number of individuals per trip, and the economic value of a trip.

Set Monthly Preference Weighting: A graphic drawing tool showing the relative monthly preference to go rafting (0-1) for the currently selected group. Click on different groups in the Trip Table to change the current group. To change the preference, click on the graphic and hold the left mouse button down while dragging the pointer over the graphic.

Set Daily Launch Policy: A graphic drawing tool showing the maximum number of launches per day for each month of the year for the currently selected group. Click on different groups in the Trip Table to change the current group. To change the preference, click on the graphic and hold the left mouse button down while dragging the pointer over the graphic.

Monthly Launch Schedule: Graphic showing the total number of launches per month for the currently selected group (computed daily launch schedule based on the monthly preference weighting, number of trips per year, and the maximum daily policy). Results shown in this graphic will change if you adjust trip type parameters, monthly preference, or maximum launches per day. Click on the Annual Total row of the Trip Table to show the total launches across all groups (trip types).

4.0   Model Structure and Assumptions

4.1   Model Overview

GCM consists of four components (Fig. 1).

A ***physical submodel*** allows the manipulation of monthly and hourly discharge and temperature releases from Glen Canyon Dam. It includes a component for simulating monthly and hourly schedules given natural patterns of inflow, various operating constraints, and other factors like power demand. A flow routing component moves water from reach-to-reach predicting changes in discharge hydrographs due to wave attenuation and tributary inputs. Reach averaged stage is predicted using rating curves derived from the STARS model. A sediment budget routes tributary inputs of fine and sand-sized sediment from reach-to-reach accounting for storage differences in eddies, main channel pools, and channel margin environments and how they change with discharge. There is a small water quality component that tracks changes in temperature and oxygen as water moves downstream and how it is altered by releases from the dam.

An ***Aquatic Productivity and Riparian Habitat*** sub-model predicts changes in aquatic macrophyte and invertebrate abundance and riparian vegetation. Benthic algal biomass is a function of flow, suspended sediment concentrations influencing light availability, and reach-averaged cross-sections. Detrital production is driven by algal biomass and includes inputs from terrestrial sources (riparian vegetation) and tributaries. Biomass dynamics of benthic insect communities is driven by benthic algal biomass and detritus concentrations but is also influenced by suspended sediment concentrations (scouring) and stage (dessication). Riparian biomass dynamics depend on reach characteristics, diurnal stage fluctuations, and responds to impacts of flow on water table height.

A set of ***Animal Population*** sub-models predicts the response of various bird and fish species to changes in riparian and instream habitats as well as variables simulated in the physical sub-model such as temperature and turbidity.. Indicator species are linked with each other and with aquatic and terrestrial productivity by modelleing the effect of food availability and predation on juvenile recruitment success. Various hypotheses regarding the effects of habitat requirements and linkages on juvenile recruitment can be simulated.

A ***Recreational/Socio-economic*** sub-model translates the effects of physical and biological changes in the system into recreational and economic costs and benefits. Costs of various diurnal flow regimes to power production at GCD are estimated using the PEAKSHAVE model. A rafting component includes a simple representation of boat movement and use patterns along the river corridor to predict camping beach demand by reach to compare with campsite availability predicted from the sediment budget. The dynamics of the rainbow trout population and fishing effort in the Lees Ferry reach is also modelled.
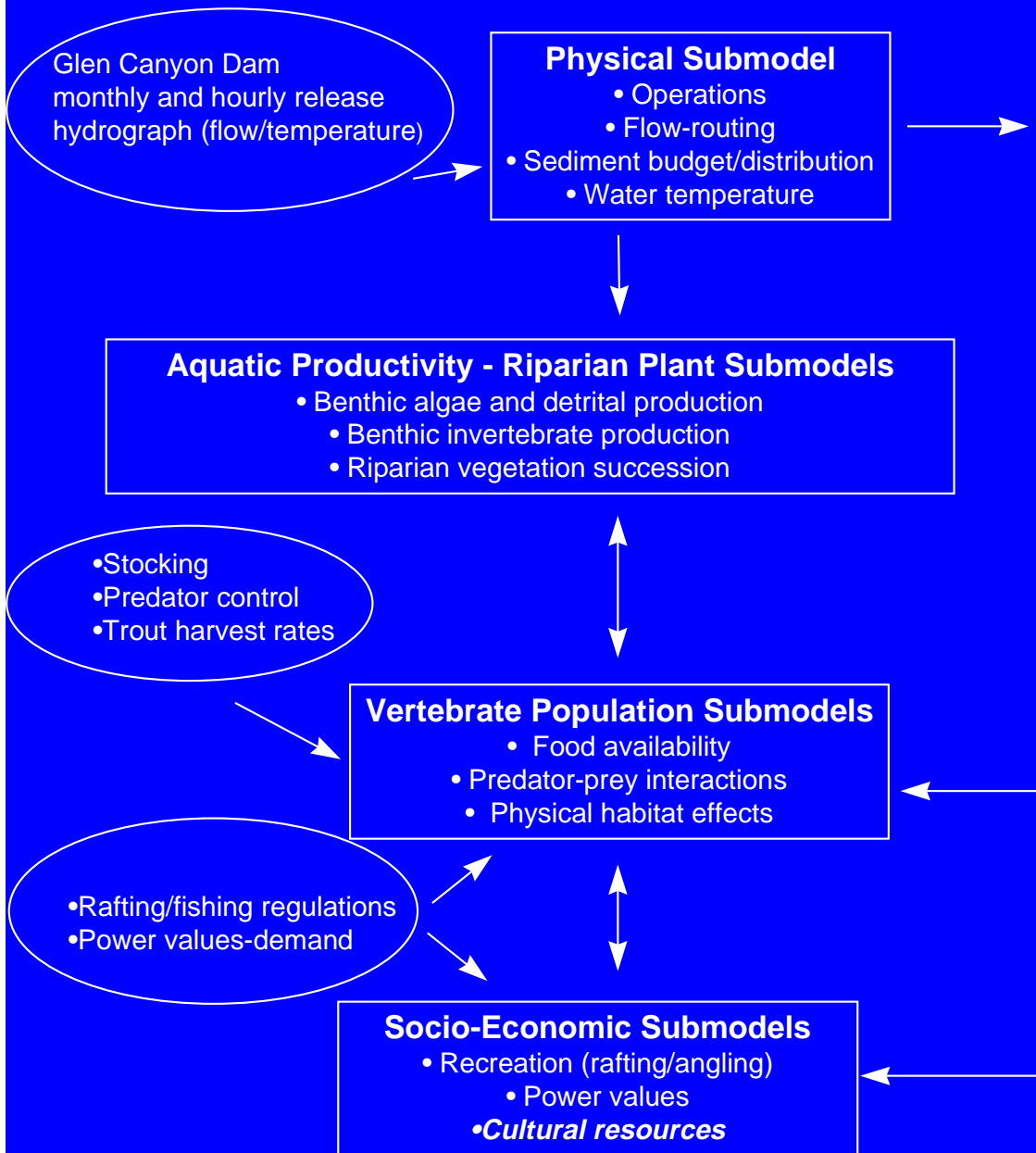
Figure 1. Submodel structure and key linkages in the GCM simulation model. A range of management options can be simulated by altering components enclosed within ovals. Items in bold italics are not modelled.

Perhaps the easiest way to visualize the overall structure of GCM is as a high-resolution food chain model, driven at the bottom of the chain by space-time variation in water flow and turbidity. Aquatic and terrestrial primary production submodels provide direct and indirect (autochtonous and allochtonous detritus) food supplies to simulated aquatic and riparian insect communities. These insect communities (represented in the model only by reach-scale biomass densities) then provide food for insectivorous fishes and birds, which are preyed upon by simulated predator populations like peregrine falcon, brown trout, and channel catfish. In fact, the food chain computations for selected animal species involve diet composition assessments that result in more of a web-like structure (juvenile fish feeding on insects, adults on small fish, mixed terrestrial and aquatic insect feeding, etc.), but a key organizing notion in the model development was to represent how the vertebrate community is supported by a production system that is variously vulnerable to impact from water management changes. However, GCM is not only a food chain model: at the top (vertebrate populations) level in the chain, we also explicitly represent possible direct impacts of a variety of habitat factors (temperature, turbidity, availability of warmed tributary and backwater areas for spawning and juvenile rearing). These factors can moderate (or exaggerate) trophic interactions, and in some cases directly cause mortality (e.g. thermal shock to juvenile fishes entering the cold mainstem from tributaries).

The wide scope of any ecosystem model entails that we must represent the dynamics of a large number of physical and ecological variables, on space and time scales ranging from a few meters and hours (e.g., effects of diurnal flow variation on benthic habitat conditions and juvenile fish behavior) up to the whole river system over decades (riparian vegetation development, dynamics of long lived species, impacts of decadal scale climate change on hydrology). While many of the key processes are occurring over short time and space scales, decisions on the efficacy of various management actions depend on long term performance over large sections of the Canyon.

The brute force modelling solution to this problem would be to pick the minimum time and space scales required to explicity model the processes and repeat the calculations over and over for decades, and over a huge number of very small patches (grids) over the entire river. There are three reasons why we didn't employ this approach in our effort.

- First, there isn't a computer fast enough to do this, and if there were, we wouldn't have the input data, for example, a 1 m grid of the whole river, to drive the detailed model.
- Second, for many of the biological processes, we would probably have to aggregate much of the detailed information to a coarser resolution. Our understanding is insufficient to use detailed physical prediction and plants and animals are integrating these effects over longer time periods like seasons anyway.
- Third, and most importantly, the multiple objectives among stakeholders and trade-offs among resources mandates that the model be interactive, allowing policy gaming in a workshop setting. Various stakeholders should be able to use the model to ask "what if?" questions to find imaginative ways to deal with conflicting objectives. The model therefore has to be computationally efficient, i.e. be capable of running long term scenarios (40-50yr) in a few minutes or less of PC time.

Given these issues and constraints, our basic modeling approach was to assume that we would have to use different time-stepping and spatial aggregation assumptions for each submodel. Our approach to the development of each submodel was to start out by discussing and thinking about the processes involved in that part of the system on very fine scales (e.g., sediment movement within a single fan-eddy complex, juvenile fish feeding along a rocky, diurnally varying shoreline), then asking how we could integrate or average over these fine-scale dynamics to produce relatively simple analytical relationships for net changes or average conditions over somewhat larger scales.

The modelled area is from GCD to near the start of Lake Mead 255 miles downstream. The river is broken down into 12 reaches that basically correspond to the Schmidt and Graf reach designation, but also includes the Lees Ferry reach and reach breaks at the Paria and LCR. We explicitly predict spatial variation in some factors much more finely. For example, sediment storage is tracked within eddy, channel margin, and pool morphologies in each reach. Some variables, like sand, algal and benthic invertebrate production, and riparian biomass are tracked within depth slices, where each slice corresponds to a 2 ft elevation increment. Processes like erosion, light availability, dessication, water availability, and flooding are driven by the elevation of the material (sand, an algal matt, tamarisk stand) relative to the water surface. For example, the rate of erosion of sand bars will be different if the bar is submerged and subjected to various hydraulic conditions, or exposed and subjected to eolian processes. Benthic algal production will vary with light availability and dessication, both of which are effected the depth of the slice relative to the water surface. Since the height of the water surface is constantly changing over time as a function of flow, cross-sectional shape, gradient, and channel roughness, we need a physical slice structure in each reach to keep track of the position of each slice relative to the water surface. In the model, we therefore created depth slices by dividing each reach-averaged cross-section into 2 ft depth increments (Fig. 2) and track the state of some variables within each of these slices as the simulation progresses.

The model simulates the period 1948 –1997, when discharge data at Lees Ferry and major tributaries became consistently available. We use a variety of timesteps depending on the requirements of each submodel. Most submodels operate on a monthly timestep, but some require hourly computations (algal biomass) while others are updated only annually (e.g. vegetation biomass).

Slice Structure of Reaches for aquatic productivity and riparian calculations and some sediment dynamics
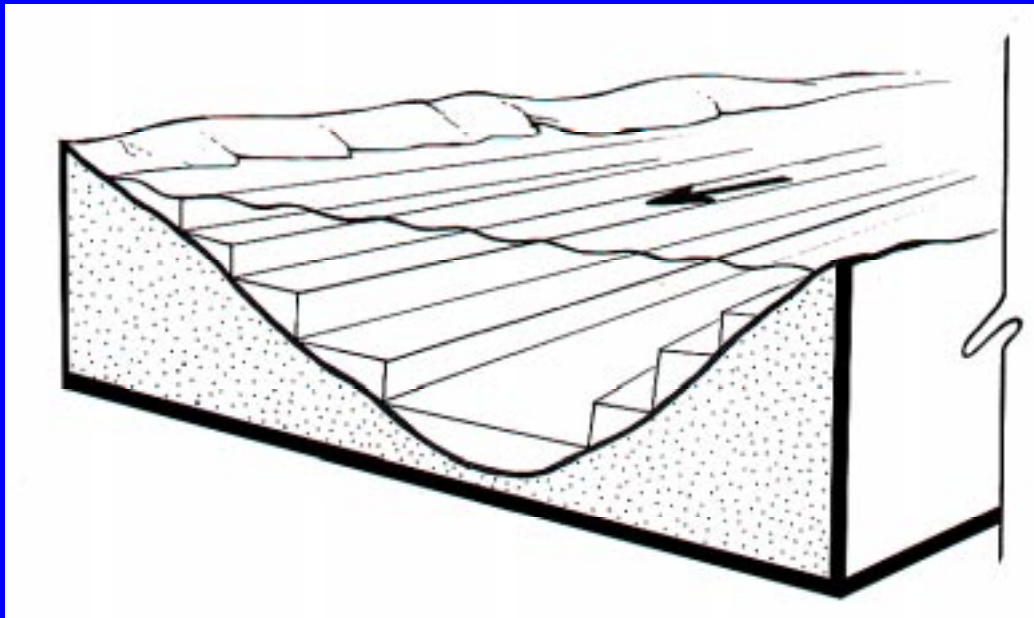

Figure 2. Spatial variation in sediment deposition and primary production variables (algal and riparian vegetation type biomasses) are represented at the scale of depth/stage "slices" (contours) within each relatively homogeneous river reach.

4.2 Physical Submodel

The physical submodel consists of four main components (Fig. 3). An operations component (Fig. 3 – orange), simulates monthly and hourly release patterns based on historical water inflows to Lake Powell, annual and monthly operating rules that support the "Law of the River", user-defined flow constraints (e.g. minimum and maximum flows, ramping rates, maximum daily flow change) and power demand. A flow-routing component (Fig. 3 – dark blue) moves water from reach to reach on an hourly timestep accounting for tributary inputs and changes in diurnal wave speed and shape, and predicts stage. A sediment budget (Fig. 3 – grey) routes sediment delivered from tributaries from reach to reach based on flow regimes and storage potential within eddies, channel margin, and main channel pool morphologies. A water quality component (Fig. 3 – purple) simulates the downstream change in average monthly water temperatures and oxygen.

4.2.1 Operations and Flow Routing

For base simulations, GCM uses the historic 48-97 monthly release volumes from GCD or volumes past Lees Ferry prior to impoundment in 1963. The use of historical releases is ideal for model validation (does the model reproduce observed changes in physical and biological resources over time?) and policy comparison (what would have happened in the past had the system been managed differently?). However, use of historic data: 1) may not provide a representative sequence of future hydrologies (e.g. due to climate change); 2) reflect future changes in upper basin water demand; and 3) allow the modification of the operating rules governing annual and monthly water releases at GCD. We therefore allow our model to be driven by output from RIVERWARE, a simulation program used by the Bureau of Reclamation (BOR) to make annual and monthly operating decisions for the Colorado River. Note Riverware is used to simulate some of the EIS alternatives like SASF and spike flow implementation following the triggering criteria.

Once a monthly release schedule for the simulation is defined, we use a model called Peakshave to predict the hourly release pattern from GCD over each month. This model determines the optimal pattern of water release from the dam to maximize power values within each month given flow constraints (EIS alternatives, maximum daily fluctuations, ramping rates, etc.), the total monthly release volume and reservoir elevation, load curves, and power prices. We summarize the hourly discharge release over each month by computing average diurnal pattern (cfs for each hour over a typical 24 hour period) for on-peak (Monday-Saturday) and off-peak (Sunday) demand periods. On-peak and off-peak periods must be modeled separately because of the concern of harmful biological effects associated with weekend low-flow periods.

On- and off-peak diurnal discharge hydrographs from GCD our routed downstream to Lake Mead using a reach-averaged model of diurnal discharge wave propagation developed by Wiele and Smith (1996). The model simulates both the change in wave speed with discharge and how the wave shape is altered as it progresses downstream. These characteristics are critical to the physical and biological environments as they effect the duration and extent of maximum and minimum stage in each reach as well as the time of day that the maximum and minimum flows occur.

Physical Submodel Overview

Historic monthly volumes OR RIVERWARE ← Hydrologic regime (climate) / Upper basin water demand / Changes to CRSP Policy

Monthly Release Schedule for Entire Simulation

Loop across all months of simulation

Seasonal/spike flow change

Diurnal flow constraints

PEAKSHAVE ← Power load/price

Hourly Release Schedule from GCD for month (average 24 hr for on- and off-peak demand periods)

Power benefits

Loop across all reaches

Tributary flow Unsteady Flow Model

Average Monthly Diurnal Discharge Patterns → STARS stage-discharge curves

GCD water release temperature

Average Monthly Diurnal Stage

Backwater/tributary hypsometric relations

Equilibrium water temperature (by month), tributary inflows/temp., heat exchange rate

Monthly tributary sediment inputs

Change in ponded tributary and backwater rearing areas

Average water temperature

Potential storage-discharge /stage relations for eddies, margins, and main channel pools, erosion rates

Change in sand storage in eddies, margins, and main channel pools

Beach inventories

Suspended sediment concentration (fines and sand)

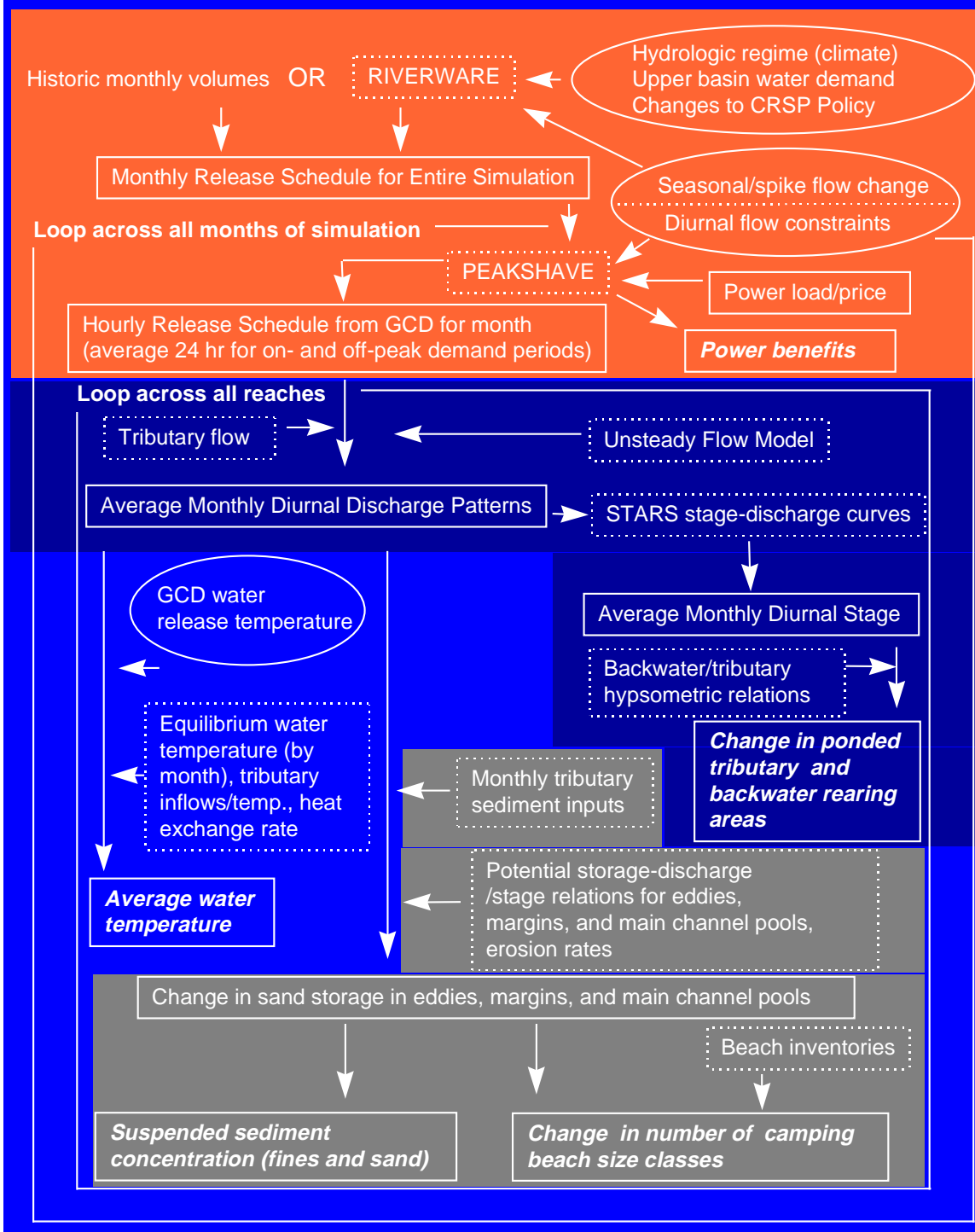*Change in number of camping beach size classes*

Figure 3. Overview of physical submodel. Text enclosed in oval shapes denote parameters that can be manipulated by the user to simulate flow and temperature management.

26

Stage in each modeled reach, predicted as a function of discharge and stage-discharge rating curves derived from the STARS model (Randle and Pemberton, 1987), is used to determine how long each depth slice (Fig. 2) is inundated over a month and to predict the area of useable backwater and ponded rearing area (Section 4.2.4).

4.2.2 Sediment Budget

A sediment budget is used in GCM to simulate the effects of diurnal flow variation and spike flows on creation and maintenance of camping beaches and to simulate temporal variation in mainstem suspended sediment concentrations effecting aquatic productivity through light attenuation and scouring. There are separate budgets for fine (silt clay) and sand (>.0625 mm) particle size classes, however almost none of the fine material is retained thus suspended fine material concentrations mirror tributary inputs. The sand budget is more involved with separate accounting of volumes in eddies, main channel pools, and channel margin environments within each reach. Model results are driven by historical deliveries of sediment through Glen Canyon and historical tributary inputs, and monthly and daily variation in mainstem discharge, and the storage relationships (Fig. 4).

Monthly tributary loads of fine (silts and clays <0.0625 mm) and sand (all particles >0.0625 mm) are based on the USGS-model for the Paria and seasonal sediment rating curves for the LCR (D.Topping, USGS, Lakewood CO, unpublished data). The maximum potential of eddies, main channel pools, and channel margin environments to store sand is discharge-dependent and predicted through a series of reach-specific sand storage relations for each morphology. For eddies, the potential to store sand increases with discharge, while for main channel pools it declines. During each model timestep, the antecedent storage conditions in each morphology predicted from the last timestep is compared to the potential under the current monthly discharge regime. If potential storage exceeds the amount of sand stored at the end of the last timestep, the volume difference can be stored if there is sufficient sediment inflow over the timestep. If the potential is less than the antecedent storage, then the volume difference is removed from the morphology, and is potentially available for storage in other morphologies within the reach or exported to the next reach downstream. A fraction of sand is eroded from each environment and is controlled by empirically-derived erosion rates.

This structure mimics some of the basic responses of different morphologies to antecedent conditions, flow, and tributary inputs. For example, under relatively low flows following a period of tributary sediment inputs, main channel pool environments will be relatively full because their storage potential is highest under low flow conditions and there has been recent sediment supplies. If the low flow conditions are maintained over a long period, upper elevations of eddy environments will be relatively depleted of sand due to erosion. If discharge is increased, storage potential in the main channel pools declines due to increased shear stress on the bottom which mobilizes material. However, eddy storage potential will increase as higher discharges increase the areaof low velocity depositional environments downstream of debris fans. Material eroded from main channel pools is therefore transferred to higher elevation eddy environments. The difference between the mass of sediment coming into the reach, and the change in storage due to these processes, which may be negative or positive, determines the mass of material that is exported from the reach which forms the input to the next reach downstream (Fig. 4).
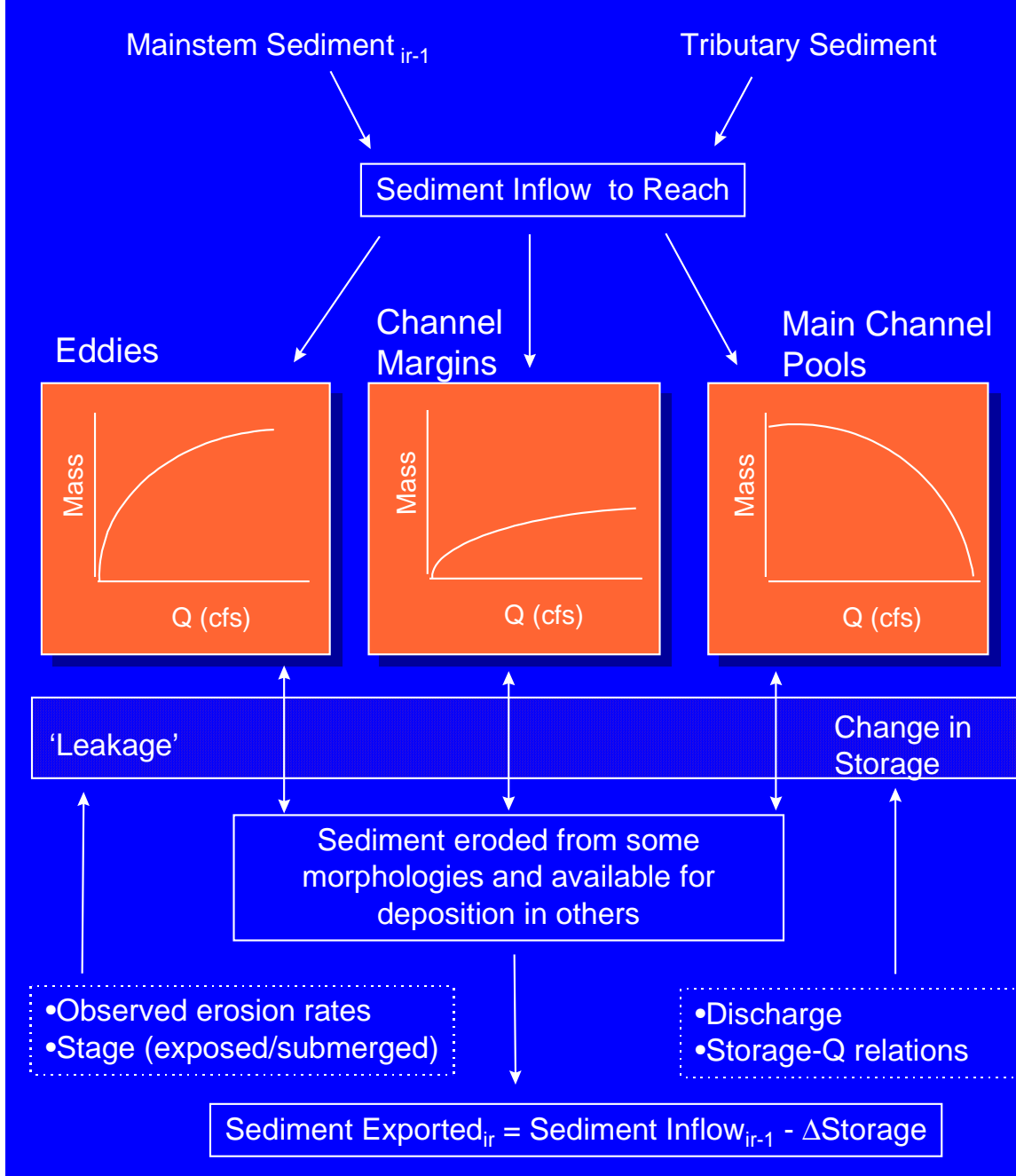
Figure 4. Overview of sediment budget with GCM physical submodel.

The key to this approach is the use of storage potential-discharge relations that were derived by a variety of methods depending on the morphology. For eddies, storage curves were developed independently for S, M, and L eddies based on the maximum potential storage computed from 15 representative sites monitored by J. Hazel and M. Kaplinski at Northern Arizona University. One reach-specific curve is developed by multiplying the number of small, medium, and large eddies estimated from air photos (K. Thompson and L. Stevens, GCMRC, unpublished data) by their respective curves and summing the total storage for a given discharge across size classes. Main channel pool storage-discharge relations were developed by Tim Randle (BOR, Lakewood, CO). Volume of main channel pools was estimated from 1984 bathymetric survey data, which occurred following the large flood and therefore represents near-maximum potential volume. The STARS model was to estimate bed velocities at different discharges for each pool. The depth at which the bed velocity is less then critical velocity required to mobilize sediment of a given particle size, estimated from transport equations, was used to determine the maximum stable depth where material can be stored under a given discharge. This procedure was repeated for each pool across a range of discharges, and reach-wide curves were created by summing all pool-specific relations within each reach. Channel margin storage is estimated using the reach-averaged cross section and an assumed stable angle of repose of 11 degrees, multiplied by the total length of channel margin deposits estimated from air photo analysis.

Empirically-derived exposed- (eolian) and submerged (tractive) -sand erosion rates (J. Hazel and M. Kaplinski, Northern Arizona University, pers. comm.) degrade sand from each storage environment. Because exposed and submerged erosion rates are different and stage fluctuates over the coarse of a simulation, we keep track of sand in depth slices within eddy and channel margin environments. This is done by decomposing the storage-discharge relation into increments corresponding to the discharge level of each slice. This is not necessary for main channel pool environments which are always submerged.

During the physical subgroup meeting, Dave Topping (USGS, Lakewood, CO.) showed some data demonstrating the importance of grain size evolution on the bed during a flood influencing downstream transport rates. Over the coarse of a mainstem flood, deposits on the bed will coarsen as smaller particles are removed preferentially due to their lower incipient motion energy requirements. This results in the hysterisis seen in mainstem sediment rating curves. Other mechanisms for this results have been proposed, such as changes in the vulnerability of sand to erosion over time; after a long period of higher flows, only the least vulnerable, sand stored in between cobbles, remains, so more energy is required to transport the same amount of material.

Regardless of the exact mechanism, to some extent our model reproduces this basic dynamic. Following a tributary flood, the main channel pool environment will be depleted due to background erosion rates and any increases in mainstem flow. A change to a higher flow immediately after a tributary input will therefore mobilize more sediment than after a longer period when the main channel environment has had more time to be depleted. The application of a constant erosion rate to progressively smaller and smaller volumes as the simulation proceeds also results in reduced downstream transport at the same discharge depending on antecedent conditions.

In any model timestep, surplus sediment is potentially stored in morphologies that have volume potential beyond their antecedent volumes at the start of the timestep. For

eddies and channel margins that have a slice structure, material is transferred only to submerged slices, with the shallowest slices receiving highest priority. In other words, the shallowest slice is filled to capacity and the surplus sediment mass is reduced by the amount transferred to the slice. The next shallowest slice is then filled, and the process is repeated until the surplus sediment supply is depleted or all storage environments are filled. In the latter case, the surplus sediment is transferred to the next reach downstream.

During subgroup discussions of eddy storage it was clear that we could not treat all elevations within an eddy equally. During high discharges, the lower elevations are thought to act more like main channel pools, with storage capacity declining with increasing discharge. During the 45,000 cfs experimental flood, the 5,000 cfs and lower eddy portions were evacuated at many of the monitoring sites. Presumably, this phenomena would scale with the flood, e.g. a 60,000 cfs flood would evacuate eddies up to the 10,000 cfs range. To model this process, we allow the user to adjust the storage potential of each slice based on the difference between the current discharge and the discharge that would just inundate each slice. When the difference is small, the slice has a maximum storage potential and as the difference increases, storage potential declines. This function is arbitrary and user-defined, but can be adjusted to simulate changes in storage in different parts of the eddy at different flood intensities, be they observed from the sand bar monitoring, or estimated from multi-dimensional hydrodynamic models.

4.2.3   *Camping Beaches*

The availability of camping beaches is an important component of the white water rafting experience in the Grand Canyon. The sediment model allows us to provide coarse statistics of temporal change in the numbers of different size classes of camping beaches (small, medium, large) in reach (termed campsite availability) to compare with campsite demand. Campsite availability in each reach is computed as follows:

1. User's define relationships between the number of beaches in a size class and the relative fullness of eddies with a stage range that is useable by campers (e.g. 25,000 – 100,000 cfs) within each reach. Existing beach inventories are used to help parameterize these functions.
2. Change in the number of each beach size class by reach over time in the model is predicted based on these relations and simulated changes in sand storage within the beach stage range of eddies.
3. Camping demand by reach and beach size class is computed from a rafting use submodel (Section 4.5.2) which uses a series of parameters defining intensity of use by different rafting groups. These parameters control the distribution of groups among reaches and the demand for the three size classes of beach.
4. Camping demand is compared to availability in each reach for each month of the simulation to identify critical reaches or times when demand for camping beaches approaches or exceeds campsite availability.

The camping beach component of the model should be considered very preliminary. The beach number–eddy fullness relations (step 1) still need to be empirically derived by combining beach inventory data with data from the eddy sand bar monitoring program (to compute the index of eddy fullness). This analysis will be complicated by inconsistencies in beach monitoring over time. The camping beach submodel also does not include the effects of vegetation encroachment on campable beach area. This could

be included in the model if changes in vegetation monitored in the GIS reaches could be related to loss of campable beach area due to vegetation. However, such an analysis does not exist, but is recommended out of this modelling exercise. Even though the camping beach submodel needs additional work, we included it at this stage of model development because of the importance of a campsite demand/availability index as a measure of sediment management success. By computing this index, users can adjust rafting use to compensate for periods of low camping beach availability.

4.2.4   Backwaters

Backwaters are considered to be important habitats for native fish species, especially in the colder water temperature of the post-dam environment. It was clear from discussions during the physical subgroup meeting that prediction of changes in backwater area under alternate flow and sediment supply regimes will be very difficult within our modelling framework. The rationale for this was that backwaters typically occur in return current channel associated with reattachment bars of constrained eddies, which are highly unstable features that vary as function of changes in sand storage and vegetative succession. These features are controlled by site-specific dynamics that cannot be modelled within the implicit spatial structure used in our sediment budget (i.e. modelling the aggregate response of all eddies in a reach, not individual eddies). We therefore opted to use empircally-derived hypsometric curves to estimate changes in backwater area by reach solely as a function of discharge. For each discharge level, there would be a fixed area of useable backwater in each reach. Such curves could be developed from digitization of air photographs with each reach-specific hypsometric relation reflecting the frequency and size of debris fans and other reach characteristics determining return current channel formation as well as antecedent conditions. These relations are static and do not predict changes in backwater areas over time due to changes in sediment deposition or vegetative succession. Similar curves could be derived to model changes in the area of ponded tributary mouths with mainstem discharge.

4.2.5   Temperature

Average monthly temperatures for each reach are computed using the Lagrange tracking method described below in Section 4.2.6. The relationship computes gains and losses of heat as water moves down the river. Predicted temperatures at the downstream boundary of each reach are driven by the release temperature from GCD, equilibrium water temperature, temperature and volumes of tributary inflows, and a heat exchange coefficient. Historical average GCD outflow temperatures for each month (B. Vernieu and J. Korn, Grand Canyon Monitoring and Research Center, Flagstaff, AZ., unpublished data) are used for the release temperatures, and the user can modify these values to simulate the effects of a selective withdrawal structure allowing warmer releases. The upstream boundary temperature for each reach (C_i in eqn. 4.2.1) is a flow-weighted average of the predicted temperature from the upstream reach and any tributary inflows. The equilibrium temperature for each month (C_{eq} in eqn. 4.2.1) is the temperature the water would eventually reach if it did not flow; it is a complex function of air temperature, direct insolation, wind patterns, and evaporation. We simply describe the seasonal variation as a table of 12 monthly values. The heat exchange coefficient (v in eqn. 4.2.1) is again a complex function of environmental conditions and has been

31

parameterized by tuning the model to observed spatial and temporal gradients in water temperature.

4.2.6 *Lagrange Tracking Method for Estimating Downstream Concentration Profiles*

One of the most difficult computational problems in river ecosystems is to represent gains and losses of materials and energy suspended in the water column, as water moves rapidly downstream (e.g. detritus, drifting insects, temperature). We use a Lagrange "sampling" method to deal with such variables: We think of taking a representative sample parcel of water entering the system each month, and following how concentrations will change in that parcel due to gains (from atmosphere, river bottom, tributaries) and losses (sinking, decomposition, heat loss) as it moves downstream. Dynamic change along each Lagrange sample track is assumed to follow relatively simple linear dynamics ($dx/dt=a-bx$, a=input rate, b=loss rate, x reset at the time when the sample parcel passes each tributary input point), for which we can obtain an analytical solution for downstream concentration changes.

The net result of processes effecting gains and losses to the sample parcel of water determine the output (concentration or temperature) at the downstream boundary of each reach in our simulation. The downstream concentration (C_{i+1}) is computed by the equation,

$$C_{i+L}=C_{eq}+(C_i-C_{eq})\exp\{-vW_iL_i/Q_i\}$$
[4.2.1]

where,
* C_{eq} = equilibrium concentration or temperature
* C_i = concentration or temperature entering the reach (a flow-weighted average value from the upstream reach and any tributary inputs)
* v = an exchange coefficient (sinking rate or heat exchange coefficient)
* W_i = wetted width
* L_i = length of the reach
* Q_i = water discharge

Eqn. 4.2.1 consists of three components:

C_{eq}: the equilibrium concentration or temperature, which would occur if the sample water parcel moved forever over an infinitely long reach at fixed gain and loss rates and no change in cross-sectional area;

C_i- C_{eq}: the extent of the departure of the equilibrium concentration/temperature from the upstream boundary condition (C_i); and

$\exp(-v*W_i*L_i/Q_i)$: a modifier on the equilibrium departure (a multiplying factor varying from 0-1), which is an exponentially decreasing function positively related to the sinking or heat exchange rate, wetted width, reach length, and inversely related to discharge. For example, the longer the reach, the closer the downstream boundary concentration or temperature will approach the equilibrium level.

Equation 4.2.1 was derived by initially formulating the change in mass within a reach over time as a difference equation,

$$\Delta M/\Delta t = RW - sWC \qquad [4.2.2]$$

That is, the rate of change in mass/temperature over time ($\Delta M/\Delta t$) within a reach will be a function of the difference between the gains due to resuspension (RW, a function of the resupsension rate and the surface it acts on, which is proportional to the wetted width) and the losses due to sinking (sWC, a function of the sinking rate, the surface this process occurs on, and the concentration, C). Note that C is a function of mass divided by the volume of water and eqn. 4.2.2 is therefore a differential equation. If we solve this equation over the period (t) it takes the water, moving at a velocity (v) to pass through a reach of length L (t=L/v) and replace any reference to mass in eqn. 4.2.2 with its concentration equivalent (C/A, where A is cross-sectional area which is equal to the volume for a 1 ft. thick section of water), we get the solution for the concentration at the bottom of the reach (C_{i+1}) given by equation 4.2.1.

4.3   Aquatic Productivity/Riparian Habitat Submodels

4.3.1   Aquatic primary production

Benthic algal communities (mainly *Cladophora* and *Oscillatoria*) are apparently the main source of food for aquatic insects in the Grand Canyon. Insect biomasses decline dramatically downstream from the area of high primary production below Glen Canyon Dam (Stevens et al. 1997), indicating that other detritus sources are insufficient to support high insect production (i.e., the system does not change from autochtonously driven to allochtonously driven, while maintaining high total food supplies for insects all along the river). That is, the whole downstream aquatic ecosystem appears to be driven by changes in aquatic primary productivity, particularly in the upper reaches.

Two main factors appear to influence algal biomass and production: (1) turbidity, which varies dramatically on seasonal and interannual time scales downstream from the Paria and Little Colorado Rivers; and (2) diurnal flow variation, which subjects algal communities in shallow waters to complex patterns of variation in light penetration and potential mortality due to dessication. Further complicating the impact of diurnal flow variation is that diurnal stage (depth) waves at Glen Canyon Dam move down through the system much faster than the water, taking about two days to move from GCD to Lake Mead (Wiele and Smith 1996). Communities near the dam are subject to deeper water during the day (which tends to reduce production due to reduced light penetration), then nocturnal drying; the net effect is that there is very little algal development in the diurnal "varial zone" and in depth slices just below this zone. But communities about 12hr wave travel time downstream see an opposite pattern: minimum stages at midday permit some primary production even when turbidity is high, and increased stage at night protects such depth slices from dessication so that there can be relatively high primary production at the lower margin of the varial zone. To model these complex relationships, we do an hourly calculation of potential primary production rate (function of depth and turbidity) and dessication time for each depth slice (Fig. 3) in each reach, for a typical 24 hr period of diurnal stage fluctuation each simulated month. Then equilibrium biomass for the slice is predicted from these typical production and dessication rates.

To represent the complex space-time pattern of algal biomass and production that likely results from diurnal production/dessication/turbidity interactions, we predict monthly average algal biomass per area, B(r,d), for a set of 2-ft depth slices (contours) d (d=1 represents bottom area from deepest point to 2 ft depth across the channel, etc.) in each reach r. Mean production per area P_r is then assumed proportional to the area-weighted mean of these biomass densities:

$$P_r = k\Sigma_d B(r,d)W(r,d) / \Sigma_d W(r,d) \qquad [4.3.1]$$

where W(r,d) is the cross-sectional width of depth slice d for a typical cross-section in reach r and k is a production/biomass scaling parameter. On monthly time scales, we assume that average biomass will satisfy the balance relation production=mortality, but we assume that (1) mortality is inversely related to the proportion of time H(r,d) that site r,d is flooded (H(r,d)=hours/day that site r,d is flooded/24), and (2) production can be limited by biomass at low biomasses, according to a saturating relationship of the form:

$$P(r,d) = P_{max}(r,d)B(r,d)/(1+P_{max}(r,d)B(r,d)/P_A) \qquad [4.3.2]$$

where $P_{max}(r,d)$ is maximum net production per unit biomass per day at site r,d and P_A is a maximum primary production per unit area in sites where B(r,d) is high enough so that production rate is not limited by algal biomass. Taking the rate of biomass change to be:

$$dB(r,d)/dt = P(r,d) - MB(r,d)/H(r,d) \qquad [4.3.3]$$

where M is a base mortality rate per biomass per day for sites that are permanently flooded, we can predict mean B when dB/dt=0 by setting P(r,d)=M/H(r,d):

$$B(r,d) = P_A[H(r,d)/M - 1/P_{max}(r,d)] \qquad [4.3.4]$$

Note here that the M/H mortality assumption causes mortality to double for each halving of H, e.g. mortality is 2M if dessication occurs for 12 hrs/day, 4H if it occurs for 18 hrs. etc. For low H or P, eqn. 4.3.4 predicts negative average biomass (daily mortality exceeds daily production for all B); in this case we set B(r,d)=0.

To apply the algal biomass prediction model (eqn. 4.3.4), we need to estimate proportions of time flooded H(r,d) and maximum daily productions per biomass $P_{max}(r,d)$. The hydrology submodel provides hourly stages S(r,h) for each reach r and hour h of the day (h=1…24), using results from the Wiele and Smith (1996) 1-dimensional wave propagation model, and the sediment transport submodel provides mean monthly turbidities by reach from which we can calculate light extinction coefficients λ_r by reach. For each depth slice d, we estimate H(r,d) simply by summing the hours for which S(r,h)>d. Daily maximum primary production rate P_{max} is taken to be proportional to the sum over daylight hours of depth-corrected hourly rates, including in the sum only those hours for which S(r,h)>d:

$$P_{max}(r,d) = K/12 \sum_{h=dawn}^{h=dusk} \exp[-\lambda_r(S(r,h)-d)] \qquad [4.3.5]$$

Here K represents maximum daily P/B for shallow water when the photoperiod is 12 hrs

and the hour summing indices "dawn" and "dusk" are adjusted seasonally for changes in photoperiod. Note that we need to evaluate eqn. 4.3.5 for a potentially large number of reaches r and depth slices d, at least once per month during simulations; to avoid unnecessary and potentially massive computational costs, eqn. 4.3.5 is evaluated for each r each month only for those depth slices d such that the light extinction effect exp(-X) is greater than 0.01; for very turbid downstream reaches, this means the eqn. 4.3.5 sum only needs be done each month for a few depth slices d. In eqn. 4.3.5. the light extinction coefficient λ_r is assumed proportional to total turbidity T_r, as $\lambda_r = \lambda_1 + \lambda_2 T_r$.

Note that the basic form of the biomass prediction relationship 4.3.4 is robust to alternative assumptions about how biomass is limited. For example, suppose we start with the assumption that P/B depends only on environmental factors such that there is no production/area limit, but that mortality rate increases with biomass. Then we would use the equilibrium of the rate equation $dB/dt = P_{max}B - MB^2/H$ to provide an approximation to the mortality rate effect. At equilibrium for this model, $P_{max}B = MB^2/H$, implying $B = P_{max}H/M$ which is similar to eqn. 4.3.4 (B proportional to $P_{max}H$, inversely proportional to M) except it does not predict a threshhold minimum for P,H below which B would be zero.

As with other trophic components of the model, a key issue is whether primary production exerts bottom-up control on production of herbivores, or can be instead be controlled through top-down grazing effects. We assume that persistent high biomass (mats) of forms like *Cladophora* implies bottom up control, i.e., the benthic algal mat must not be subject to very high grazing rates (due perhaps to chemical defenses of the algae, or to grazing insects being prevented from feeding on open surfaces by high predation risk from fish). Extensive direct grazing would be obvious, in the form of patchiness in algal biomass at the scale of a few cm ("worm trails" and other grazing impact signals). Absent such signals, we assume that algal production moves through the food chain mainly via (1) consumption of epiphytic diatoms growing on the macroalgae, and (2) detritus production and consumption of this detritus by insects that spend most of their time in protected microhabitats (e.g., web spinners under rocks). Detritus production per unit area is assumed proportional to primary production, and "instantaneous" downstream profiles of detritus concentration are predicted each week using an exponential profiling procedure based on Lagrange tracking of water masses downstream (Section 4.2.6) while accounting for additions from the bottom (and side terrestrial sources), decomposition, and grazing removal rates.

4.3.2   *Riparian plant communities and production of allochtonous detritus and insect inputs to the river*

Our aim in this submodel is to represent broad changes in shoreline vegetation types due to changes in flow regimes, and changes in contributions of detritus and insects from shoreline communities to the aquatic ecosystem. We simulate biomass dynamics for five main vegetation types at depth slices within each reach (Fig. 3). There are dynamic equations for annual growth-competition relationships, and for monthly mortality due to flooding and drying. Each vegetation type is assumed to be capable of growing on a subset of substrate types and range of elevations above current high water (representing depth of water table). Monthly flooding and drying impacts are represented by an arbitrary curve relating mortality rate to duration x depth of flooding (and duration of dessication); such curves can be "sketched" by model users using a

mouse-driven entry interface along with information about substrate types upon which each vegetation type can grow.

We assume detritus and terrestrial insect production from riparian communities to be proportional to relative biomass and area occupied by each vegetation type, with large differences among vegetation types. Generally, faster-growing vegetation is assumed to produce more detritus and insects. Lacking direct data on insect population dynamics and production, we in effect assume that insect populations remain close to equilibrium with (track changes in) vegetation biomass. Production rates of terrestrial insect drift into the aquatic system are set so as to fit measured drift concentrations for 1994-1995, roughly 10% of drift contribution from aquatic insects (Shannon et al. 1996).

Main differences in dynamics by vegetation community type are assumed to be the following:
(1) *desert shrubs*—grew naturally above seasonal high stage mark, now at moderate densities 3m and more above annual average high water mark; very slow biomass growth (10-20%/yr.) and low production of detritus, insects.
(2) *mesquite-acacia*—grew in narrow band just above high water, now slowly dying out at most original sites; also very slow biomass growth and detritus/insect production.
(3) *upland grass*—locally occupied wide band above high water mark, especially in shady (by canyon walls and orientation) areas with older sand deposits from very large historical floods; rapid growth but relatively low biomass and detritus production.
(4) *salt cedar-willow*—mainly an invader community on sand bars following elimination of seasonal flooding, mainly 0.5-3 m above average high water mark; locally very dense and productive of detritus and insects.
(5) *Equisetum-Carex* shoreline marsh—again an invader community on sandy areas from present high water mark to about 1m higher, dense root mats help anchor sand; also locally very dense especially in lower reaches, productive of detritus and insects.

The salt cedar-willow community is of particular concern for future ecosystem management; it is variously described as a wonderful nesting and feeding habitat for birds, a key source of insect production, an unnatural eyesore, and an annoyance for campers (very dense stands are virtually impassible). That is, there is no clear concensus about whether it represents a good or bad change in the ecosystem.

Changes in relative biomass density $B_{p,r,d}(t)$ (a 0-1 biomass scale per unit suitable habitat) for plant type p in reach r, cross-sectional depth (stage) slice d are simulated with the following discrete logistic equation for time steps t of one year:

$$B_{prd}(t+1)=B_{prd}(t)[1+G_{prd}(t)]S_{prd}(t)+s \qquad [4.3.6]$$

Where,

$S_{prd}(t)$ is the product of all monthly survivals through flooding events and inappropriate water table levels during year t, s is a seeding input rate (biomass colonization rate) and the logistic relative growth rate Gprd(t) is given by:

$$G_{prd}(t)=r_p[1-B_{prd}(t)-\Sigma_k a_{kp}B_{krd}(t)] \qquad [4.3.7]$$

In this growth function, r_p is an intrinsic rate of biomass increase for plant type p, and the a_{kp} represent competition coefficients (effect of unit of biomass of plant type k on the growth rate and carrying capacity for plant type p, $a_{pp}=1$). In practice, for plant type definitions used in baseline simulations the competition coefficients have little effect; the plant types are "segregated" in habitat use by strong survival effects (S_{prd}) caused by assuming different tolerances/preferences for height above the water table.

The water table height $W_r(m)$ for each month m is set as a simple average of the last month's water table height and of the mean diurnal river stage $D_r(m)$ for each reach each month, as:

$$W_r(m+1)=0.5W_r(m)+0.5D_r(m) \hspace{4cm} [4.3.8]$$

That is, water table height is assumed to "track" changes in river stage with a modest time delay, rising somewhat slower than the water level and decaying with a lag of around one month during periods of falling stage. In practice, this assumption has little effect on predictions for most water management scenarios. For natural system "replays", violent seasonal stage variations cause much larger survival S_{prd} effects than would changes in water table depth , and most managed system scenarios do not involve large month-to-month changes in mean stage $D_r(m)$.

While these equations appear to give reasonable predictions of biomass development and hence total reach-scale relative biomasses for substrate types that are stable on time scales of decades (rock, ancient elevated sand bars, boulder and cobble areas), they may predict too rapid a change in total reach-scale biomass for water management scenarios that cause sudden, substantial increases in sand bar area near the present high water line (e.g. "beach-building" floods of somewhat larger magnitude than the 1996 experimental flood). That is, since the model is not keeping separate account of each substrate area by "age" of origin or deposition (a very complex data gathering and simulation problem), it will "suddenly" assign biomasses $B_{prd}(t)$, predicted from past dynamics on already established sand bars, to the newly deposited area. Fortunately, this effect is relatively small in most scenarios, especially since flows that can produce large new sand areas also cause a substantial "reset" of all $B_{prd}(t)$ in affected depth slices (flooding survival effect).

We tried to develop rough estimates of detritus production from riparian vegetation as contribution to allochtonous production in the aquatic community. While estimates of detritus production per unit area from riparian vegetation do not appear large enough to sustain substantial aquatic insect production, there was considerable debate about two issues. First, allochtonous inputs may enter the river from a much wider "catchment" than just the riparian zone (canyon walls, canyon rim, etc.), making it impossible to predict total inputs from any simple areal assessment of riparian vegetation. Second, there are local "hotspots" (mainly eddies and backwaters) of detritus delivery and potential insect production, at spatial scales smaller than we simulate. Such sites could store pulses of low-quality (leaves, large woody debris) detritus from tributary flood events long enough for that detritus to be made available to the aquatic insect community through bacterial/decomposition processes.

We have developed preliminary estimates of allochtonous carbon inputs delivered from wider catchment areas. Total drainage areas for each reach are computed from a database of tributary drainage areas from T. Melis (GCMRC, Flagstaff, AZ). A fixed

amount of carbon per unit of drainage area is delivered per spate event (8.5 g C/spate/m^2 drainage area) based on the 4300 g/m2/sec AFDM CPOM measured at Sycamore Creek, AZ (Fisher and Minckley 1978). The number of spates for each month over the period of simulation for all reaches is determined from rainfall at the Phantom Ranch rainfall gage (>1 inch of rain falling consecutively is considered a spate).

4.3.3 Aquatic insect production

Aquatic insects form the primary food supply for most fishes and some riparian bird species (e.g., ducks, swallows). During model development, there was considerable debate about whether the natural system had a productive insect community (and hence about whether it could have supported a substantial fish community). At present there is a dramatic downstream decline in insect densities below the clear water Glen Canyon Reach, suggesting no significant allochtonous replacement of detritus food supplies from terrestrial sources within the Canyon. But observations in the Cataract Canyon area upstream from Grand Canyon indicate a high and diverse biomass apparently supported by detritus sources in the Colorado River headwaters.

Our modeling approach was to divide insect biomass into three main biomass categories: grazers (mainly *Gammarus*, in clear water reaches), detritovores (mainly Chironomids and *Simulium*), and combined drift. We calculate mean monthly biomass densities of grazers and detritovores for each river reach, then use the Lagrange sampling method (Section 4.2.6) to calculate downstream changes in mean drift density. Input rate to the drift is assumed proportional to biomass density, and loss rate from drift is assumed to occur at a constant instantaneous rate (constant fraction of drift biomass lost per time to settling, emergence, and predation).

Benthic insect biomass dynamics are represented by monthly difference equations at the reach spatial scale; no attempt is made to simulate biomasses by depth slices within reaches, due to likelihood that movement processes (crawling, drifting, etc.) among slices are fast enough to prevent substantial slice-scale variation from developing over time. Also, benthos sampling data do not indicate clear trends in biomass with depth, except for substantial biomass reduction in diurnally dried varial zones (we assume zero production in these zones) and lower average biomass in deeper sites since more of these sites have unstable sand substrates.

For each invertebrate type s (grazer, detritovore) in each reach r, we update monthly (m) biomass density (g/m^2 ash free dry wt.) $B_{sr}(m)$ using the difference equation:

$$B_{sr}(m+1)=B_{sr}(m)[1+g_{sr}(F_{sr}(m))-m_{sr}(m)] \qquad [4.3.9]$$

where $g_{sr}(F_{sr}(m))$ is a biomass growth function dependent on food density $F_{sr}(m)$ and $m_{sr}(m)$ is a mortality rate dependent on temperature, predator abundances, diurnal dessication, and (in extreme situations) turbidity. Also, between months of rising mean stage, B is "diluted" by assuming animals rapidly spread over the wider river width available; between months of falling stage, animals along the drying river margin are assumed to die (rather than contribute to increases in biomass density B by moving to remaining wetted areas).

The biomass growth function $g_{sr}(F_{sr}(m))$ was derived by thinking initially about filter feeders (dominant in most river reaches), and assuming that animals compete locally

38

within and upon the substrate for limited delivery rates of detritus to that substrate. We assume that similar local "delivery" rate mechanisms apply to production of the epiphytic algae (diatoms) that appear to be the main food supply of grazers (macro algae like *Cladophora* and *Oscillatoria* appear not to be grazed directly, or at least not enough to cause noticeable effects like hedging or patchiness). Within the limited "grazing arena" at the substrate, we suppose that g has the product form efc, where c=effective food concentration in the arena, and f=filtering/scraping rate (volume or area/time), and e=food conversion efficiency. The problem then is to predict c as a function of overall food concentration $F_{sr}(m)$ in the environment and of exchange/production/loss processes between c and F. We assume mixing processes result in dc/dt=MF-rMF-fB/V, i.e. to have input rate proportional to F with instantaneous rate M, non-grazing loss rate proportional to F with rate rM (for detritus, r represents "resuspension" rate relative to "sinking" rate M), and feeding loss rate fB/V where f has units of volume per biomass per time and V is the effective volume of the grazing arena. We then assume that c reaches equilibrium quickly with respect to B and F (on time scales of hours to days) so that we can solve for c by setting dc/dt=0. Substituting this variable speed splitting solution for c into the rate product efc then results finally in the overall relationship:

$$g_{sr}(F_{sr}(m))=efMF_{sr}(m))/[rM+fB_{sr}(m)/V] \qquad [4.3.10]$$

Here the hyperbolic decreasing term Fsr(m))/[rs+fBsr(m)/V] represents the fast variable solution for c (density of food locally available to animals immediately at the substrate where they are competing). Note that in the case s=grazers, we think of $F_{sr}(m)$ as proportional to macroalgae biomass density, so that it represents algal concentration on macrophyte growth sites not accessible to grazing due to predation risk or other factors.

To simplify the estimation of parameters in eqn. 4.3.10, we directly specify only e, r, M, baseline equilibrium values F_o, B_o and mortality rate m, and maximum biomass growth rate r_o at low densities (this growth rate is r_o=efF$_o$/r-m). Substituting these "knowns" into eqn.'s 4.3.9 and 4.3.10 with B(t+1)=B(t) results in estimates of effective f and V. In fact this method allows us to make arbitrary choices for M as well (only product MV appears at equilibrium, so changing M just rescales estimate of effective arena volume V), and to think of the "resuspension" fraction r as a way of representing concentrating mechanisms such as quiet backwaters that support some insect production even where overall water column concentrations of detritus F (or bottom concentrations of algae) would be too low to support any production.

Why assume the relatively complex competition function 4.3.10 rather than assuming growth rates simply proportional to overall detritus or algae concentrations in/below the water column? First, all the available data suggest that food supply is indeed important to benthic insect abundance (strong downriver gradients, etc.). But if we simply assume that growth rate is proportional to overall food density $F_{sr}(m)$, we end up predicting that g should be either large enough to always predict B(m+1)>B(m), or always low enough so B(m+1)<B(m), i.e. we end up predicting either unlimited population growth or decline. In simple food limitation models, increase in B results in decrease in F and hence population-limiting feedback. But especially for F=detritus in a large, fast flowing river, the relatively low benthic biomass simply cannot affect overall food concentrations significantly, even over substantial downstream distances. The "grazing arena" density effect (reduced food density in the immediate environment where animals feed) is actually a very parsimonious way to introduce food-mediated density dependence (and hence population regulation) into the model.

Mortality rate $m_{sr}(m)$ is assumed to consist of two components, m_o+m_1. We assume the baseline "natural" rate m_o would occur in the absence of fish and bird predation, due to various physiological problems and to maturation/emergence. The predation rate m_1 is assumed to vary on interannual time scales with abundances of fish. m_1 is parameterized by assigning each vertebrate predator species a baseline proportional contribution to m (i.e. a component of m_1) when the vertebrate species is at baseline (1993) abundance, such that m_o consists of overall m times whatever proportional contribution is not accounted for by modeled predators. Then m_1 is varied over time in proportion to ratios of predator abundance to baseline predator abundance. This approach allows us to easily examine various hypotheses about top-down versus bottom-up control of predation effects (to effect bottom-up control, we set the relative predator contributions to total m at low values to model the idea that predation rate has little additive effect on m; to model top-down control, we set the proportions so most of m is directly accounted for by predators).

4.4   *Vertebrate Population Submodels*

We attempted to develop a fairly flexible population dynamics model for representing reach-scale interannual variation in a large set of vertebrate indicator species that account for most of the predatory biomass in the ecosystem (baseline 15 species). This population dynamics model has two main parts (Section 4.4.1): (1) an age structure and (optionally) biomass accounting system for abundance of age 1 and older animals, where we can "turn off" some time delay effects (e.g. age at maturity) and biomass accounting to provide only simple numbers accounting (N next year=survivors plus new recruits) for species with simple life histories and/or limited life history data; and (2) a complex recruitment model relating age 1 recruits to parental egg/hatchling production, food supply, predation risk, and physical habitat variables such as temperature and tributary rearing area. The concept in this derivation is that most important population dynamics events and limiting factors operate mainly on juveniles during their first year of life, before they find "secure" ways to make a living (become large enough to use a wide variety of physical habitat conditions and to avoid high predation risks).

The key component of this submodel is the recruitment relationship, which we derived (Walters and Korman 1998) by thinking about how evolution has shaped the behaviors of small juveniles to deal with three main problems: (1) finding secure resting habitats safe from predation, (2) finding enough food to grow enough to eventually mature, and (3) incurring high predation risk while feeding (due to small body size, lack of experience with predators, etc.). Following arguments in Walters and Juanes (1993), we assume that juvenile animals try to spend as much time as possible in safe refuge sites (shallow shorelines, under protective rocks and vegetation, etc.), and hence are restricted to forage in relatively small spatial "foraging arenas" near these refuge sites. Spatial restriction of foraging in turn implies that there can be locally intense exploitation competition for food, i.e. overall food supplies in the environment may be large but food densities may be reduced substantially in the foraging arenas when juvenile densities in these arenas are high. We assume that juveniles adjust time spent foraging (and dispersing to find less crowded sites) so as to maintain some basic "target" growth rates ("optimized" through natural selection). Analyses of food production/exchange rates for foraging arenas then imply that time spent in foraging arenas, and hence time at risk to predation in such arenas, should increase about linearly with local juvenile density. Hence if predation risk is proportional to time spent foraging, juvenile mortality rates

should increase linearly with juvenile density. Linear density-dependence in instantaneous juvenile mortality rates is the basis of the classic, widely used Beverton-Holt (1957) relationship, which for fish predicts the widely-observed phenomenon of eventual recruitment being largely independent of egg deposition (i.e., to be "limited" by factors other than egg deposition) over wide ranges of parental abundance.

The recruitment relationship derived from these arguments has explicit terms for resting (refuge) area and foraging arena physical size (essentially refined measures of effective habitat size), predation risk per time foraging which may in turn depend on habitat variables like temperature and turbidity, and apparent food density which may also depend on habitat factors like turbidity. In the simulation we generate time varying food supplies (mainly aquatic and terrestrial invertebrates for the indicator vertebrate populations considered so far), and indices of predation risk based on changes in relative abundance of potential vertebrate predators (abundances of other species included in the list of index species). A convenient feature of the derivation is that predation risk and food effects appear only as a ratio P/F (predator abundance/food density), so we can "lump" habitat effects on recruitment into two habitat effect types: (1) effects on the risk ratio via effects on predator avoidance and feeding efficiency, and (2) effects on potential food competition via total sizes of accessible foraging arenas.

Due to lack of microscale foraging behavior data on juvenile fishes, we have been unable to address one potentially serious weakness in the recruitment formulation. Our derivation is based on the assumption that behavior of each species of juvenile fish results in a unique foraging arena for that species, within which there can be strong intraspecific competition for food. Effects of interspecific competition are included in the calculations only through large-scale effects of multispecies exploitation on reach-scale densities of invertebrate food types. We thus assume that there has been strong selection for microscale behavioral differences among species (diurnal times of feeding, specialization in prey species choice, etc.) to avoid intense exploitation competition within small foraging areas. But in reality, there could be important interspecific competition among juvenile fishes in some microhabitats, particularly between native and exotic species in warm backwater and shoreline sites. Thus the model may underestimate impacts of exotic fishes in the ecosystem, though we already assess these effects to be potentially very large through predation on juvenile native fishes alone.

We simulate a time-varying (reach, month scale) set of physical habitat capacity/risk/food availability indices including: temperature, turbidity, area of warm tributary/backwater habitat, diurnal stage change (reduces availability of shoreline refuge habitats for small fish), and total wetted area. A graphical user interface allows us to "sketch" hypothesized relationships between these habitat factors and components of the recruitment relationship (habitat size available to juveniles, risk ratio), and on adult growth rates.

Lacking reliable total abundance estimates for most of the vertebrate species, particularly exotic fishes like carp and channel catfish, we internally scale population model parameters to spatial relative abundance indices based on methods like electrofishing, beach seining, and visual counting. Taking 1993 as a base index year, we calculate recruitment scaling parameters so as predict constant abundance over time (equilibrium abundance) if predation risk, food density, and physical habitat factors remain at 1993 levels; available trend data suggest that most vertebrate populations

were in fact not changing rapidly around that time. For each juvenile vertebrate species, we specify 1993 baseline estimates of the proportion of juvenile mortality due to each modeled predator type, and proportion of different food types (benthic insects, algae, terrestrial insects) in the juvenile diet. Then the risk ratio (predators/food) calculations are scaled so as to give user-specified maximum juvenile survival rates (in absence of competition) when predator and food relative abundances are at 1993 levels, and to give proportional increases/decreases with proportional changes in relative abundances away from the 1993 baseline levels.

4.4.1 Computational Details for Vertebrate Population Submodels

To simplify the following presentation of population dynamics relationships, we supress subscripts for reach and species. It is to be understood that all age-structure accounting relationships (for age 1 and older animals) are done at system-year scale (once per year for each species), and all recruitment relationships (egg/hatchling to age 1) are at reach-month scale.

The age structure population dynamics accounting is based on the Deriso (1980)-Scnnute (1987) delay-difference equation structure used widely in fisheries assessment (see derivation in Hilborn and Walters 1992). For animal ages 1 to an age at maturity k, numbers at age are propagated using a simple survival relationship $N(a+1,t+1)=S_jN(a,t)$ where S_j is an annual juvenile survival rate. For age k and older animals, we propagate total numbers N (summed over all ages, ignoring age-specific differences in survival rate) and adult biomass B using the delay-difference relations:

$$N(t+1)=S_aN(t)+R(t+1) \qquad [4.4.1]$$

$$B(t+1)=S_a[AN(t)+(rho)B(t)]+w_kR(t+1) \qquad [4.4.2]$$

where ,
  t is time in years
  S_a is adult annual survival rate (constant except for harvesting/control effects)
  $R(t+1)$ is age k recruitment, number of animals
  A, (rho) are Ford-Brody body growth model parameters
  w_k is mean body weight at maturity

It is not necessary to propagate these equations at the reach spatial scale since we do not assume reach-specific differences in age 1+ growth and survival rates (except for time varying harvest effects on S_a for rainbow trout in the reach just below Glen Canyon dam, where most of the rainbow population is found). The age 1 numbers entering the juvenile age accounting each year (leading at age k to total recruits R) are calculated as a sum over reaches of recruitment rates by reach.

Adults using each reach (proportion of N,B based initially on historical data and then updated in relation to simulated recruitment success by reach over years) are assumed to produce eggs/hatchlings E(t) proportional to biomass, E(t)=eB(t) where e=eggs/adult biomass. Derivations in Walters and Korman (1998) imply that we can predict the number of age 1 recruits resulting from E(t), while accounting for monthly changes in predation risk related to food supply and growth, by a Beverton-Holt (1957) function of the form:

$$N(1,0)=E(t)S_{egg} \qquad\qquad [4.4.3]$$

$$S_m(m)= \exp[-K_1 v_m H_r(m)P(m)/F(m)] \qquad\qquad [4.4.4]$$

$$N(1,m+1)=N(1,m)S_m(m)\,/(1+K_2\,(1-S_m(m))N(1,m)/\,(v_m H_f(m))] \qquad\qquad [4.4.5]$$

where,
  S_{egg} is egg survival rate, assumed constant
  m is month of age (after hatching) m=1…12
  v_m is relative vulnerability of m-month old juveniles to predation
  $S_m(t)$ is maximum (low density) survival rate over the month
  K_1,K_2 are scaling constants that depend on units of measurement (see below)
  $P(m)$ is an index of total predation risk per time foraging
  $F(m)$ is a weighted (by diet composition) index of food density
  $H_r(m)$ is a function defining relative (0-1) variation in the risk ratio effect
   (P/F effect on survival) with changes in physical habitat factors
  $H_f(m)$ is a function defining relative (0-1) variation in usable foraging habitat
   (foraging arena size) with changes in physical habitat factors

There are two key components in eqn. 4.4.4: trophic linkage to predation risk and food availability via the risk ratio P(m)/F(m), and linkage to physical habitat factors that affect both predation risk and food competition via the habitat functions H_r and H_f.

The P and F functions are weighted sums over predators and food types of predator and food specific relative risks/opportunities. In initializing each simulation for baseline year 1993, we scale these functions so that P=1, F=1 if predator and food abundances identical to 1993 values reoccur in other simulation years. So for example, if we have assumed a particular predator accounts for 20% of the juvenile mortality in the 1993 baseline situation, we take its contribution to P in other years to be 0.2B(t)/B(1993), where B(t) is predator biomass in year t. Contributions to F are calculated the same way. We attempted a spreadsheet trophic modeling exercise to see if we could replace such relative predation and feeding rate calculations with dimensional mortality rate parameters based on absolute estimates of predator abundances, feeding rates, and diet compositions. This exercise revealed really discouraging gaps in basic abundance and feeding data, particularly for key exotic species. The relative P and F calculations allow us at least define clear alternative hypotheses about possible predation and food impacts, without pretending that we can quantify each of the component calculations required to justify any particular hypothesis.

In the first (1993 baseline) simulation year of each scenario, we calculate the equation 4.4.4 H, P, and F monthly factors for every indicator species, then use these to calculate K_1 and K_2 so that N(1,12) (age 1 recruits) will just balance assumed natural mortalities of older animals provided habitat, predation, and food conditions remain constant. K_1 is estimated over reaches as a single, non-spatial factor, using observed relative abundances by reach to weight the spatially varying H, P, and F factors. But the K_2 "calibration" is done by default on a reach-by-reach basis, so the K_2 parameter can represent habitat capacity effects besides those modeled explicitly with H_f. This default calculation can be turned off by model users (initialization calculates single abundance-weighted average K_2 over reaches), to see if explicitly recognized habitat relationships included in calculation of H_f can explain observed spatial distribution patterns (this two stage optional calculation was necessary particularly in early model development in

order that we could "drive" the submodels for particular species with reasonable spatial relative abundance estimates for predator/competitor species, and work through the habitat linkage parameterization in some systematic way across species).

K_1 in fact represents a "compensation parameter", in the sense that the product $S_m(m)$ over months represents maximum survival rate of eggs to age 1. Model users can either specify this maximum survival rate directly, or can assume the maximum survival rate to be $K^*(R_o/E_o)$, where R_o/E_o represents survival rate needed to produce a population equilibrium at the baseline (1993) egg production rate E_o. In the second approach, K^* represents the ratio of maximum survival rate at very low population density to the survival rate for a balanced population. There are no empirical data on K^* for Grand Canyon vertebrates (no stock-recruitment data); based on comparative studies of fish recruitment relationships (Myers and Barrowman 1996) we have advised users to assume K^* values on order 3-10.

Each "habitat linkage function" $H_r(m)$ and $H_f(m)$ is calculated as a product of effects over habitat factor values for month m. (Habitat factor values available in the simulation for each reach, month include temperature, turbidity, max-min stage, wetted area, and warm tributary+backwater area). Model users can sketch functions of the form $h(V_k)$, where $0<h<1$, and V_k is the value of the kth habitat factor in month m (e.g., V_1=max-min stage, V_5=turbidity); V scales are set relative to 1993 baseline values. Each H is then just the product $h(V_1)h(V_2)\ldots$ over those factors V for which the model user has sketched some relationship (h=1 for "inactive" V's). By defining H as a product of h(V) effects (rather than, say, a sum of effects), we assume each habitat factor has a strong effect independent of other factors (a high f value for one habitat variable cannot "compensate" for a low value for another variable, e.g., having a large habitat area cannot compensate for poor thermal conditions). In the same model interface, users can sketch the v_m function (0-1 relative values) defining how sensitivity to both H and P/R varies with age over the first year of life; we initially allowed definition of a separate v_m function for each habitat factor, but we found this greatly complicated the functional specifications without substantially improving our ability to represent alternative hypotheses about importance of various habitat factors.

4.5   Socio-Economic Submodels

A number of socio-economic indicators are effected by the operation of Glen Canyon Dam. In GCM, we consider the direct economic costs of alternate flow regimes on power revenues generated from GCD. We also model the effects of flow changes on white water rafting in Grand Canyon and flow/temperature effects on trout angling in the Glen Canyon reach immediately below the dam. Our rafting index is a comparison of campsite demand and availability, while our angling indices track changes in total catch, catch rates, and effort. To date, we have not attempted to translate these indices into monetary values but may do so in the future by incorporating recreation-economic models developed by BOR (D. Harpman, BOR, Lakewood, CO., pers. comm.).

We have not modeled the effects of dam operation on cultural resources in Grand Canyon. Perhaps the most important issue here is the erosion of archeological sites by arroyo cutting in short ephemeral streams that drain the terraces of the river corridor (Hereford et al. 1993). The reduction of sediment load and elimination of the annual flood in the post-dam era have reduced the elevation of depositional environments and are hypothesized to intensify arroyo cutting and accelerate the exposure of archeological

sites. The second issue concerns the potentially intensified erosion of banks (due to reduced sediment load from dam operations) which support very high (>300,000 cfs) terraces where archeological sites are located. The third issue concerns changes in the abundance and distribution of ethnobotanical plants due to dam operations. The first two issues require relatively detailed predictions based on multi-dimensional hydrodynamic models which are too detailed to be used in our long-term, whole-reach assessment. Changes in ethnobotanical resources may be coarsely simulated in future efforts by associating each plant species with one of the five riparian community types that we do model, and then computing an ethnobotanical-weighted biomass index based on the relative abundance of each community type.

4.5.1 Power Values

The value of electricity varies substantially over time depending on the demand for power. Demand is higher during the summer and winter when required for cooling and heating and is higher during the day when businesses are open, and lower at night and on weekends. Changes in daily and monthly operation of GCD associated with different release alternatives will have no effect on the annual power generation (i.e. the same amount of water will be passed through the turbines over the coarse of a year) but will affect the schedule of electrical output and hence its value (NRC 1996).

The PEAKSHAVE model (Harpman and Rosekrans 1996) is used in our simulation to predict the hourly release pattern from GCD and power values generated for each month given a set of operating constraints (minimum and maximum daily flow, maximum daily upramp and downramp rates, maximum daily flow change) and a total monthly release volume. Estimates of the monthly value of power are based on 1996 spot marked price data that represent current conditions in the regional power market (Harpman 1998). Power value estimates over a long-term simulation assume no change in base generation of resources effecting demand and price (i.e. a short-run economic analysis).

The cost of various mitigative flow constraints (e.g. MLFFA, the modified low fluctuating flow alternative) are computed by comparing monthly power values with those generated under the No Action alternative, the historic operating regime allowed when plant operations were not restricted by ramping rates and other constraints intended to benefit downstream ecology. In a representative water year (11.3 million acre-feet released from GCD) under the No Action alternative, the model estimates that Glen Canyon Dam will produce approximately $70 million worth of energy (in 1996 dollars). By comparison, under the current MLFFA policy, GCD will produce $64 million, equivalent to an annual loss of $6 million or 8.6% (Harpman 1998).

4.5.2 White Water Rafting

Sediment deposits along the Colorado River in the Grand Canyon serve as campsites for rafting groups. Since completion of GCD in 1963, there has been a noticeable loss of suitable campsites principally due to erosion, lack of replacement with incoming sediments, and vegetative succession..

The rafting component of GCM compares the demand and availability for campsites on a reach-by-reach basis for each month of the simulation. Sediment budget predictions of reach-wide changes in sand storage for eddy environments are used to calculate the

change in the number of beaches in small, medium, and large beach size classes. The rafting use submodel predicts changes in campsite demand for each beach size class based on a number of parameters that the user can manipulate including the: 1) maximum number of trips/yr for each of four group types (commerical -oar and -motor, private-oar, research-motor); 2) maximum number of launches/day at Lees Ferry; 3) average number of persons and the length of a typical trip for each group; and 4) the relative preference for rafting in different months over the year.

Campsite demand for each rafting group in each reach for each month of the simulation is computed as follows:

1. Total trip length for each group is divided by the distance from Lees Ferry to Diamond Creek to compute the average daily travel distance and the upstream/downstream limits of each daily travel section.
2. The average number of launches per day for each month (for each group) are computed by distributing the total number of trips/year based on the monthly preference weighting assigned by the user. If the resulting daily launch schedule exceeds the maximum number of launches per day (a user-defined constraint), the extra launches are redistributed to the next preferred months.
3. Campsite demand is computed for each reach based on the daily launch schedule and the overlap of travel sections and model reach breaks. For example, 5 launches per day of commercial-motor trips results in a demand of 5 large campsites per day in each travel section. This is equivalent to 150 campsite-days in large campsites per month. The reach-specific value may be greater or less than daily travel section value depending on the overlap between the reach and daily travel section.
4. Campsite demand by reach and size class is compared to campsite availability predicted by the sediment budget component of the model (Section 4.2.2).

In critical reaches, low camping beach availability results in heavy use of some beaches during the peak of the rafting season. The rafting use model predicts the frequency of such events based on launch schedules (simulated in step 2) above) and existing beach inventories. In the current version of GCM, beaches identified during the 1991 beach inventory (Kearsely and Warren 1992) are populated over the coarse of a simulation each month based on the average daily launch schedule of each group, the size of the site (determining which groups can use it), and a preference value for each campsite. The preference reflects the desirability of each site which accounts for proximity to points of interest (archeology, hikes, creeks,..), camping quality, and logistics. Campsites in each travel section (the length of river a group travels in an average day) are filled in order of preference. During situations of high use the model double-books some sites (two groups using the same site in one day) in reaches which low beach availability (critical reaches). For this component of the rafting use model, site number and size in each reach is held constant so intensity of use at each campsite reflects the implications of the current rafting use policies on the 1991 camping beach inventory. Other beach inventories can easily be substituted in the analysis.

The economic value of rafting each month of the simulation is computed by multiplying the number of trips for each group by the monthly average value of commercial and private trips (Bishop et al. 1987, 1989; Boyle et al. 1993).

4.5.3   Trout Angling

The Glen Canyon rainbow trout fishery, located in the first 15 miles downstream of GCD, is one of only two blue-ribbon stream fisheries in Arizona and is used by over 19,000 anglers each year (NRC, 1996). Many flow/temperature discharge regimes being considered for beach/habitat building and recovery of native fish species are believed to be potentially harmful to this fishery. Large daily fluctuations associated with maximum power value generation also maximize the loss of the aquatic food base due to algal/aquatic insect dessication. Higher temperature releases, which could be achieved through the construction of a selective withdrawal structure, have the potential to increase trout competitors and predation on juvenile trout. Although whirling disease has currently not been detected in trout in the Grand Canyon, it may already be present but kept in check by low water temperatures. Increasing water temperatures potentially increases the risk of a whirling disease outbreak.

The Glen Canyon reach trout population is simulated using the same framework applied to other species in GCM, but in addition, we explicitly model stocking rates and angling mortality. The trout angling submodel predicts changes in total catch, catch rate, and effort over time. Angling mortality (u) is computed by specifying a monthly set of catchability (q) and effort rates (Effort) in the catch equation (Hilborn and Walters 1992):

$$u = 1 - Exp(-q * Effort) \hspace{3cm} [4.5.1]$$

Catchability is assumed to increase with fish size and varies seasonally according to use-defined patterns. Effort can be held constant over a simulation or vary dynamically based on the biomass of vulnerable fish according to:

$$Effort = (EffortMax * RelBio \char`\^ Slope) / (HalfMax \char`\^ Slope + RelBio \char`\^ Slope) \hspace{1cm} [4.5.2]$$

where, Effort is the predicted number of angler days for the month, EffortMax is the maximum possible effort for that month, RelBio is the ratio of vulnerable biomass in the current timestep to the vulnerable biomass during the initialization year (1993), Slope is the steepness of the effort-biomass relationship, and HalfMax is the ratio of vulnerable biomass (current/1993) that results in 50% of EffortMax. The regional economic value of the Lees Ferry trout fishery is compute by multiplying the predicted number of angler days in each month by the average monthly value of angling (Bishop et al. 1987, 1989; Boyle et al. 1993).

When effort is allowed to vary dynamically, the model is able to reproduce the broad changes in relative trout abundance and utilization that have occurred since construction of GCD, with some obvious errors in the timing of events due to not including some dynamic effects like time-varying stocking rates and changes in angler preferences and behaviour (anglers now release most fish, whereas until the late 1980s they exerted quite high removal exploitation rates).

5.0   References

Beverton, R.J. and S.J. Holt. 1957. On the dynamics of exploited fish populations. Fisheries Investment Series 2. Vol. 19. U.K. Ministry of Agriculture and Fisheries, London.

Bishop, Richard C., Kevin J. Boyle, Michael P. Welsh, Richard M. Baumgartner, and Patricia C. Rathbun. 1987. *Glen Canyon Dam Releases and Downstream Recreation: An Analysis of User Preferences and Economic Values*. Glen Canyon Environmental Studies Report No. 27/87. Madison, Wisconsin: Hagler Bailly Consulting, Inc., 1987, pp. 188. Springfield, Virginia: National Technical Information Service, NTIS No. PB88-183546/AS

Bishop, Richard C., Curtis A. Brown, Michael P. Welsh, and Kevin J. Boyle. 1989. "Grand Canyon Recreation and Glen Canyon Dam Operations: An Economic Evaluation." In *W-133, Benefits and Costs in Natural Resource Planning: Interim Report 2,* edited by Kevin J. Boyle and Trish Heekin. Orono, Maine: Department of Agricultural and Resource Economics, University of Maine, July 1989.

Boyle, Kevin J., Michel P. Welsh, and Richard C. Bishop. 1993. "The Role of Question Order and Respondent Experience in Contingent-Valuation Studies." *Journal of Environmental Economics and Management* Vol. 25 No. 1 (July 1993):80-99.

Deriso, R.B. 1980. Harvesting strategies and parameter estimation for an age-structured model. Can. J. Fish. Aquat. Sci. 37: 268-282.

Fisher, S.G., and W.L. Minckley. 1978. Chemical characteristics of a desert stream in flash flood. Journal of Arid Environments 1:25-33.

Harpman, D.A., and A.S. Rosekrans. 1996. Modeling hourly operations at Glen Canyon Dam Colorado River storage project, Arizona. GCPS09 version 1.0. U.S. Department of Interior, Bureau of Reclamation.

Harpman, D.A. 1998. Assessing the short-run economic cost of environmental constraints on hydropower operations at Glen Canyon dam. Land Economics (*in press*).

Hereford, R., Fairlye, H.C., Thompson, K.S., and J.R. Balsom. 1993. Surficial geology, geomorphology, and erosion of archeologic sites along the Colorado River, eastern Grand Canyon, Grand Canyon National Park, Arizona. U.S. Geological Survey, Open-File Report 93-517.

Hilborn, R. and C. Walters. 1992. Quantitative fisheries stock assessment and management: choice, dynamics, and uncertainty. Chapman Hall, NY.

Kearsley, L., and K. Warren. 1992. River campsites in Grand Canyon National Park: Inventory and effects of discharge on campsite size and availability. National Park Service in cooperation with Glen Canyon Environmental Studies.

Myers, R.A., and N.J. Barrowman. 1996. Is fish recruitment related to spawner abundance. Can. J. Fish. Aquat. Sci. 52: 223-232.

NRC. 1996. River Resourse Management in the Grand Canyon. National Academy Press. Washington, D.C. 226 p.

Randle, T.J., and E.L. Pemberton. 1987. Results and analysis of STARS modeling efforts of the Colorado River in Grand Canyon. U.S. Department of Interior, Bureau of Reclamation. NTIS No. PB88-183421/AS.

Shannon, J.P. Blinn, D.W., Benenati, P.L., and K.P. Wilson. 1996. Organic drift in a regulated desert river. Can. J. Fish. Aquat. Sci. 53: 1360-1369.

Schnute, J. 1987. A general fishery model for a size-structured fish population. Can. J. Fish. Aquat. Sci. 44: 924-940.

Stevens, L.E., J.P. Shannon, and D.W. Blinn. 1997. Colorado River benthic ecology in Grand Canyon, Arizona, USA: dam, tributary, and geomorphological influences. Regulated Rivers: Research & Management 13:129-149.

Walters, C.J. and F. Juanes. 1993. Recruitment limitation as a consequence of natural selection for use of restricted feeding habitats and predation risk taking by juvenile fishes. Can. J. Fish. Aquat. Sci. 50:2058-2070.

Walters, C.J. and J. Korman. 1998. Linking recruitment to trophic factors: revisiting the Beverton-Holt recruitment model from a life history and multispecies perspective. Rev. Fish. Biol. Fisheries (In press).

Wiele, S.M. and J.D. Smith. 1996. A reach-averaged model of diurnal discharge wave propagation down the Colorado River through the Grand Canyon. Water Resources Research: 32(5), 1375-1386.